

Equivalence between in-house and conventional EM immunity test techniques

Christo Nicholls



UNIVERSITEIT • STELLENBOSCH • UNIVERSITY
jou kennisvenoot • your knowledge partner

Thesis presented in partial fulfilment of the
requirements for the degree of Masters of Science
(Engineering) at the University of Stellenbosch

Supervisor Prof H.C Reader

March 2007

Declaration

I the undersigned hereby declare that the work contained in this thesis is my own original work and that I have not previously in its entirety or in part submitted it at any university for any degree.

C.Nicholls

Date

**Copyright ©2008 Stellenbosch University
All rights reserved**

Abstract

Keywords: Electromagnetic Immunity measurement techniques, Equivalence

Conventional immunity tests are both time consuming and costly. There is thus a reasonable interest in relatively quick, but accurate and cost effective, in-house pre-compliance test techniques within an engineering design-house. This thesis provides information on the equivalence between in-house and conventional immunity test techniques.

Three techniques were evaluated, namely: 1. E-field radiation with a log periodic antenna (conventional test technique); 2 E-field radiation with an in-house designed and constructed modified TEM cell (in-house test technique); 3. Current injection using a complete off the shelf EMCO current probe device (in-house test technique).

After the transfer data of the EMCO probe was verified, the modified TEM cell design, construction and equivalent measurement tests were performed. These tests revealed that within the respective bandwidth of interest, the devices produced results that are equivalent to each other within 0.9dB. Hence equivalence between in-house and conventional test techniques is possible.

Opsomming

Sleutel woorde: Elektromagnetiese Immuniteits Metings,
Ekwivalensie

Konvensionele immuniteits toetse is beide duur en tydsaam. As gevolg van hierdie faktore is daar dus 'n groot behoefte vir relatiewe vinnige, maar tog akurate en lae koste in-huise voorlopige goedkeurings immuniteits toetse in die ingenieurs bedryf. Hierdie tesis verskaf inligting pertinent rondom die onderwerp van ekwivalensie tussen konvensionele en in-huise immuniteits tegnieke.

Drie tegnieke was ge-evalueer, naamlik: 1. E-veld Radiasie met behulp van 'n Log-Periodiese antenna (konvensionele tegniek); 2. E-veld Radiasie met behulp van 'n in-huis ontwerpte TEM sel (in-huise tegniek); Stroom induksie met behulp van 'n kommersieel beskikbare stroom probe genaamd EMCO (in-huise tegniek).

Nadat die oordrags funksie van die EMCO probe bevestig was, die TEM sel ontwerp en gebou was, was die ekwivalensie metings uit gevoer. Die gevolgtrekking wat gemaak kan word uit die meetings is dat die ekwivalensie tussen die drie meet tegnieke verskil met maksimum 0.9dB binne die gewenste bandwydte. Dus is ekwivalensie tussen konvensionele en in-huise meet tegnieke moontlik

Acknowledgements

I would like to start off by thanking the Lord Jesus Christ for granting me this opportunity to not only expand the horizon of my technical knowledge, but also for the privilege of meeting new people and hence strengthening the glue that keeps things together in my life, namely relationships.

Secondly, I would like to commend Prof. Reader for defining a very abstract concept in the borders of our country, namely the art of mentorship. WELL DONE. Also for his conscious decision to trust in my ability in completing this project successfully.

Then to Wessel Croukamp and his WHOLE team, THANX!!!

Second last, to Trevor Kirsten and the TSO management team, thank you for your faith and financial support.

Lastly, to my wife for her continuous support and understanding, thanks a million!!!

CONTENTS

Figures.....	i
Tables.....	i
1 INTRODUCTION	1
2 LITERATURE REVIEW AND THESIS FOCUS.....	3
2.1 Introduction.....	3
2.2 Bulk Current Injection	4
2.3 E-field Radiation	4
2.4 BCI versus E-Field Radiation	5
2.5 Focus of Thesis	9
2.6 References	9
3 VERIFICATION OF EMCO PROBE TRANSFER IMPEDANCE	11
3.1 Introduction.....	11
3.2 Verification of the transfer impedance data.....	13
3.3 Discussion of the verification results	17
3.4 References	20
4 MODIFIED TEM CELL	21
4.1 Introduction.....	21
4.2 Theoretical Design of the modified TEM Cell.....	23
4.2.1 Taper Design	23
4.2.2 Design of the Uniform Area.....	29
4.3 Practical Construction of the Modified TEM Cell.....	33
4.4 Test and Evaluation of the modified TEM cell.....	36
4.4.1 Evaluating the Modified TEM cell taper effectiveness.....	36
4.4.2 Evaluating the Uniformity of the Modified TEM Cell.....	38
4.5 Conclusion.....	41
4.6 References	42
5 PROOF OF EQUIVALENCE.....	43
5.1 Test Methodology	43
5.1.1 Calibration of the Modified TEM Cell	45
5.1.2 Calibration of the EMCO Current Probe	52
5.2 Proof of Equivalence	54
5.2.1 The Process Followed to Proof Equivalence	54
5.2.2 Equivalence Measurements.....	55
5.2.3 Discussion on the Equivalence Measurement results.....	57
6 CONCLUSIONS AND RECOMMENDATIONS	59
Appendix A.....	62
Appendix B.....	63
Appendix C.....	64
Appendix D.....	68
Appendix E	69

FIGURES

Figure 2-1: Experimental set-up for practical analyses of radiation versus injection (after [2]).....	8
Figure 2-2: Detailed geometry of the parallel plate structure	8
Figure 3-1: A picture of the EMCO Current probe	12
Figure 3-2: Method one used in setting-up the EMCO probe as a two port network	14
Figure 3-3: Method two used in setting-up the EMCO probe as a two port network.....	14
Figure 3-4: Pictures of the constructed CISPR16 metal cabinet used. The lower picture shows the open cabinet for clarity.....	16
Figure 3-5: A comparison between the measured and supplier provided EMCO probe transfer impedance data.....	17
Figure 3-6 Schematic of the test set-up and related results linked to the investigation on the unwanted resonance with the small EMC cabinet used to calibrate the EMCO probe	18
Figure 4-1: Graphical representation of the S11 of the exponential taper as per equation 3.1 above	25
Figure 4-2: A graphical representation of the exponential tapers of the TEM cell	26
Figure 4-3: A cross sectional view of the TEM cell identifying the dimensions of the TEM cell that are parameters of the higher order modes of the parallel-plate related cavity or wave guide	30
Figure 4-4: An illustration of the slots on top of the Taper part of the TEM cell	34
Figure 4-5: The uniform area of the constructed Tem cell with the three test loops and uniformity test plate	35
Figure 4-6: Measurement set-up used to execute the TEM cell taper S11 measurement..	36
Figure 4-7: Reflection coefficient measurement results of the constructed TEM Cell.....	37
Figure 4-8: The test set-up for the uniformity tests performed on the TEM cell	38
Figure 4-9: Results obtained from the TEM cell uniformity measurements	39
Figure 5-1: Graphic outlay of the complete process followed to prove equivalence between the three EMI measurement techniques	44
Figure 5-2: The test set-up used to establish the consistency of the generic test set-up probe.....	46
Figure 5-3: Test set-up used to acquire the data is used as the reference data for the calibration of the TEM cell.	48
Figure 5-4: Test set-up used to perform the calibration process of the TEM cell.....	50
Figure 5-5: Test set-up to capture the calibration data of the EMCO probe	52
Figure 5-6: The test set-up for the measurements performed to investigate the equivalence between the three EMC test methods	55
Figure 5-7: Graphic representation of the equivalence measurement results	58

TABLES

Table 4-1: Table summarising the width and height dimensions of the exponential taper .	28
Table 4-2: Summary on the calculated values of the cut-off frequencies of the higher order TE and TM modes in the TEM cell	31
Table 4-3: Summary of TEM cell uniformity measurements	40
Table 5-1: Summary of generic test set-up consistency measurement results.....	47
Table 5-2: A summary of the results recorded that as the reference data for the calibration of the Tem cell	49
Table 5-3: Input RF power calibration values for the TEM cell.....	51
Table 5-4: Summary of Calibration data captured for EMCO probe	53
Table 5-5: Measurement results captured for three measurements performed to investigate the equivalence	56

1 Introduction

Electronic devices for various reasons either cause electronic noise pollution or are susceptible for it. This noise has the potential to interfere with the performance of other devices present in the same operational environment. To ensure that electronic devices do not negatively pollute their environment, or become negatively influenced, various electromagnetic compatibility (EMC) standards such as IEC and Military standards were written. Besides informing the industry on what the global EMC acceptance levels are for electronic devices in specific environments, these standards also address the following EMC related issues, namely:

1. The type of test that need to be performed.
2. The test procedures that must be followed.
3. The acceptable test equipment that must be used.

Besides the conventional EMC test equipment that is being used, various forms of in-house test equipment is also used within the industry, e.g. Current probes and TEM cells. The in-house test equipment is generally

used to perform pre-compliance testing. However, after successful pre-compliance testing, conventional EMC test equipment is used for the final acceptance testing. This route is normally followed for cost and time saving purposes. In order to perform acceptable and trustworthy in-house testing the equivalence between the in-house and conventional test equipment must be quantified. The focus of this thesis is to investigate the equivalence between the conventional and in-house immunity test equipment.

Chapter 2 surveys the research performed in the area of in-house versus conventional testing. Chapter 3 provides detail on the verification of the transfer impedance data of the EMCO probe used to perform bulk current injection. The work continues into Chapter 4 where the detailed construction and evaluation of a modified TEM cell is discussed. The results obtained from the evaluation of the TEM cell, EMCO probe and conventionally used log periodic antenna, acts as the input for the discussion on the equivalence between the proposed in-house versus the conventional immunity test methods, which is captured in chapter 5. The document is concluded in Chapter 6.

2 Literature Review and Thesis Focus

2.1 Introduction

Electromagnetic immunity (EMI) tests are performed on electrical and electronic equipment to determine their level of immunity against unwanted electrical noise in their operational environment. These tests are currently performed utilizing two methods: E-field radiation and bulk current injection (BCI). In the subsequent chapters a summary of literature reviewed on BCI, E-field radiation techniques and equivalence between BCI and E-field radiation is presented. Thereafter a brief outline of the focus of thesis in the context of this literature is provided.

2.2 Bulk Current Injection

The philosophy behind bulk current injection is to inject a known common mode current unto a specific area of interest, e.g. equipment cable looms used in aircraft platforms [3]. The conventional test set-up linked to the BCI technique consists of a RF power source and a calibrated current probe.

One of the outstanding advantages of the BCI technique is that relatively low RF power can induce currents in wire bundles that would require very high-radiated RF power to induce the same power [4]. However, one of the main criticisms linked to BCI is the fact that current distribution on the individual wires in a bundle is not always the same as those induced by using the E-field radiation method [4].

2.3 E-field Radiation

E-field radiation as with BCI is also a technique to test the EMI level of an electronic device. The basis of the E-field radiation technique is that the device under test (DUT) is illuminated by a uniform plane wave at various frequencies and field intensity levels. Conventionally the E-field radiation test set-up consists of an antenna and a DUT that is placed within the far field of the antenna where a uniform plane wave is present [2]. The reason why uniformity of the plane wave is critical is purely for test repeatability reasons. In addition to the conventional E-field radiation method alternatives to the use of an antenna exists, namely: Gain horns, Parallel Plates and TEM cells [5]. The Gain horn operates well above a few MegaHertz, where the parallel plate performs as well, below a few MegaHertz. However the major draw back of these techniques is the fact that they both radiate electromagnetic energy into the surrounding space, which interferes with the actual measurements [5]. The TEM cell, as opposed to these techniques, contains the EM field inside the transmission cell. It is also extremely broadband in frequency, being effectively limited only by the waveguide multimode frequencies associated with the cell size [5]. Thus, due to the broadband characteristics and design control on the associated

modes the TEM cell was chosen as one of the pieces of equipment that was used to perform equivalent EMI tests within the context of this thesis

Myron L. Crawford first introduced the TEM cell concept in 1974 under the auspices of the National Bureau Standards [5]. The main characteristics of the TEM cell (as per [5]) can be summarised as follow:

- a. *The cell consists of a section of rectangular coaxial transmission line tapered at each end.*
- b. *The line and tapered transitions have a nominal characteristic impedance of 50 ohms along their length to ensure minimum voltage standing wave ratios (VSWR).*
- c. *The electromagnetic field is developed inside the cell when RF energy is coupled to the line from a transmitter connected at the cell input port.*
- d. *A matched 50 ohm termination is connected to the output port.*
- e. *The fields inside can be monitored using special electric and magnetic field probes as described in detail in [6].*

2.4 BCI versus E-Field Radiation

Based on the information found in the literature, the research can be divided into two main categories: theoretical and practical. The theoretical analyses compare field excitation and BCI on a bundle of wire analytically [1]. For the theoretical investigation the wire bundle is modelled as a multiconductor transmission line, which is treated as a multiport device [1]. In order to determine the equivalence of radiation versus injection the currents induced onto the wire, by both sources, are compared. It is however important to now that from a physical point of view radiation and injection have different coupling phenomena: *“radiated excitation is inherently distributed, while injection is typically a localized phenomenon. This consideration highlights the fact that in general radiation and injection produces different current distributions. However, if the objective is electromagnetic immunity tests of equipment connected at one end of the wire bundle (using any of the two*

methods), the equivalence of the induced current distribution is insignificant” [1]. This is because it is only the current that is physically distributed on the equipment that causes unwanted coupling within the equipment. Therefore the equivalence of the two excitation methods is ascertained with reference to the currents induced at the line terminations, i.e. at the input terminals of the equipment under test (EUT).

The theoretical analysis [1] found that in stating the analytical equivalence, controlling the injection probe with a voltage depending on several parameters (frequency, line length, clamp location and wave characteristics) is implied. To determine equivalence at the input terminals of the EUT, specific conditions, namely that the voltages at the input terminals for both the radiation and injection must be similar must be adhered to. Given these conditions a realization of a practical BCI measurement is difficult, due to the frequency-dependent weighting functions that modify the original spectrum of the interference.

The theoretical analysis of [1] finds that:

Radiation and injection has different current distributions. To state analytical equivalence, the need to control the current probe is imperative to match specific current-profiles. This implies the need for modulating the injected power (linked to the radiation source) to the complex frequency functions (a parameter of the current probe), therefore the theory is not sufficient for a final and univocal judgement of the effectiveness of “Radiation vs. BCI”.

As part of the practical analysis in [2] the following hardware is used: A parallel plate, H-field probe, current probes, BCI probe and terminated test wires. The distance from an antenna where the far field begins is generally defined as $R=2(D)/\lambda$, where R = far field distance from the antenna, D = dimensions of the largest antenna aperture and λ = wavelength of the transmitted or received signal. In the far field of the radiation antenna the E-field is uniform. One of the disadvantages then is that the EUT must be in the far field area of the radiation antenna to ensure experimental repeatability. To circumvent this and to create a uniform E-field and a test

environment that will allow repeatable tests, a parallel plate is utilised.

Although a parallel plate is utilised in [2], it is possible to use other techniques to create uniform E-fields, e.g. a TEM cell.

To ensure that the wanted E-field is generated beneath the parallel plate, effective impedance matching between the source generator, parallel plate and load is necessary. The physical dimensions of the plate as well as height of the plate above the ground level determine the test frequency range. The input generator level is determined by considering the losses due to the matching networks, voltage divider rule and the equation for an E-field. Once the input generator voltage is determined, the uniformity of the E-field beneath the parallel plate is established.

With the uniformity of the E-field established, test wires are inserted between the parallel plates. These wires are terminated with different impedances to ground. The chosen impedance simulates real life condition e.g. 1Ω for a near short condition, 50Ω for typical electronics and electrical loads and 270Ω for sensitive electronic equipment. Figure 1 depicts the experimental setup used to investigate the equivalence between radiation and injection in [2].

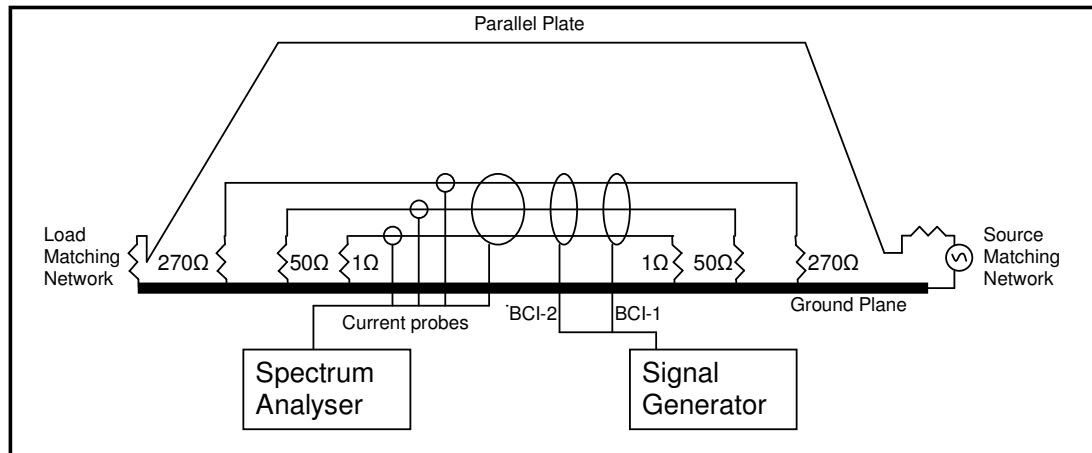


Figure 2-1: Experimental set-up for practical analyses of radiation versus injection (after [2])

The detailed geometry related to the parallel plate as per Figure 2-1 above is depicted in Figure 2-2 below.

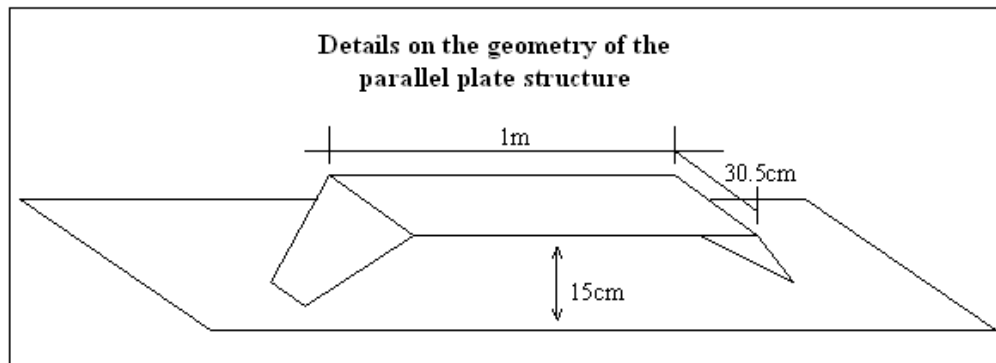


Figure 2-2: Detailed geometry of the parallel plate structure

To measure the field-to-wire induced currents, the wires are set-up under the top plate as in figure 1 and illuminated with the uniform E-field. Next the overall bundle current induced onto the wires from the parallel plate is measured with all three wires in the probe. Lastly the currents induced on the individual wires are measured with their related probes.

To obtain the BCI induced currents at each frequency, the current value obtained from the overall bundle measured in the parallel plate method is

injected using the BCI clamp over the 3-wire bundle. With the current probes over the individual wires, the wire currents induced from the BCI clamp at each frequency for each of the 3 wires are measured. Equivalence between the radiation and injection method is ascertained by comparing the measured current value on the individual wires due to the parallel plate method and due to the BCI method.

The practical analysis of [2] concludes that:

At frequencies where the test wire lengths $< \lambda/4$ the BCI and radiation method correspond within 2dB with each other.

2.5 Focus of Thesis

The focus of this thesis is to ultimately comment on the equivalence between in-house and conventional EMI test methods. The thesis addresses this issue by reporting on equivalence tests performed between a modified Transverse Electromagnetic (TEM) cell and BCI as the in-house test methods versus the conventional E-field test method.

2.6 References

- [1] S. Pignari, F. G. Canavero, "Theoretical Assessment of Bulk Current Injection Versus Radiation", IEEE Trans. On Electromagnetic Compatibility, Vol.38, No.3, p469, August 1996
- [2] D.H. Trout, "Investigation of Bulk Injection Technique by Comparison to Induced Currents from Radiation Electromagnetic Fields", NASA, George C, Marshall Space Flight Center, MS EL23, MSFC, AL 35812
- [3] Mr Gavin.D.M. Barber, "The use of Direct Current Injection (DCI) techniques for aircraft clearance", 10th IEE Conference, p199
- [4] David A. Hill, "Currents induced on Multiconductor Transmission Lines by Radiation and Injection", IEEE Trans. On Electromagnetic Compatibility, Vol. 34, No.4, p445, November 1992

[5] Myron L. Crawford, "Generation of Standard EM Fields Using TEM Transmission Cells", IEEE Trans. On Electromagnetic Compatibility, Vol.EMC-16, No.4, p189, November 1974

[6] F.M. Greene, "Design and Calibration of E and H Field Probes for HF Band Application", Proc. Dep. Defence Electromagnetic Res. Workshop, Washington, D.C., pp.50-76, Jan.1971

3 Verification of EMCO probe transfer impedance

3.1 Introduction

In the context of EMI testing, two predominant methods exist, namely radiating the unit under test with a uniform E-field or injecting a current onto it. For the latter method a current probe is utilised. For the purpose of this research an EMCO current probe depicted in Figure 3-1 (a commercially off the self product with a frequency bandwidth of 10Hz up to 1GHz) was used. The detailed specifications for this product are listed in Appendix E of this document. . In general terms these common mode (CM) probes are used as comprehensive investigative emission testing devices. This is done by placing the probe onto all external cables connected to the DUT, and then measuring the frequency and level of the CM currents. These currents can be directly related to measured emissions.

In the context this thesis the EMCO probe was used as an alternative means to inject current onto the device under test (DUT). Therefore the verification of the EMCO probe's transfer impedance is important in insuring the integrity of the measurements. The subsections to follow will describe the verification process.

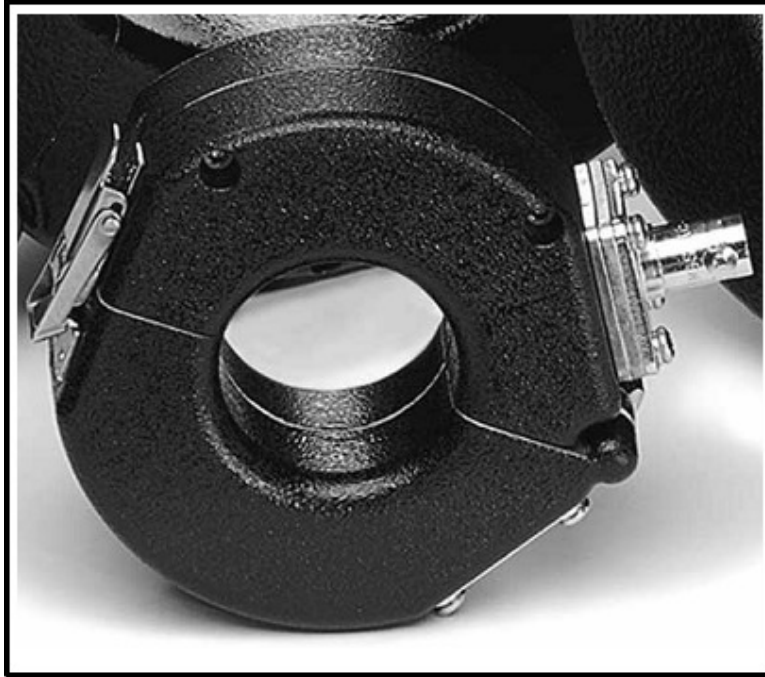


Figure 3-1: A picture of the EMCO Current probe

3.2 Verification of the transfer impedance data

The verification process of the transfer impedance data can be summarised as follow:

1. Set-up the EMCO probe as a two port network
2. Capture the Scattering-parameters (S-Parameters) of the EMCO probe
3. Convert the S-parameters to the related Z-parameters (Impedance characteristics of the network).
4. Calculate the transfer impedance (Z_t) of the EMCO probe using the known Z-parameter values
5. Compare the measured Z_t of the EMCO probe with the supplied version

In setting-up the EMCO probe as a two port network two methods were followed as illustrated in Figure 3-2 and Figure 3-3 below.

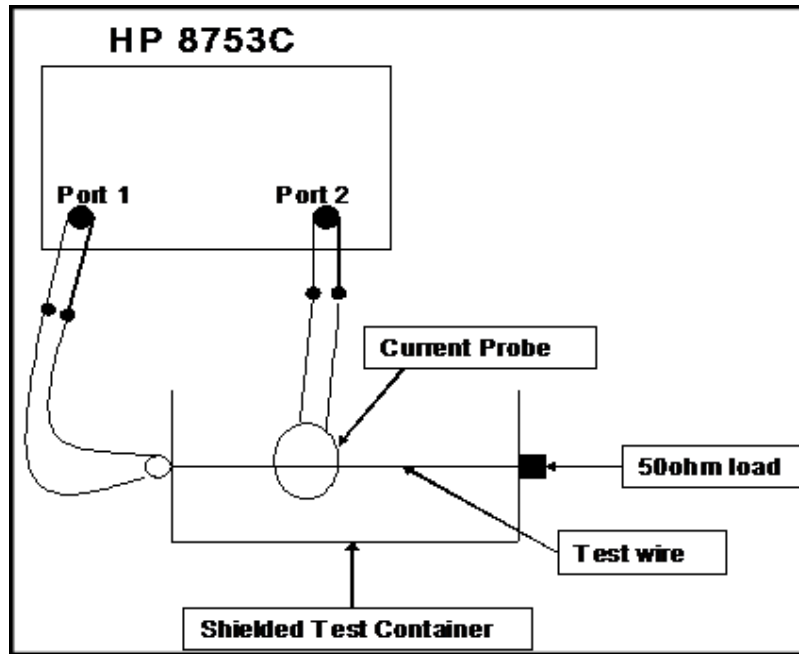


Figure 3-2: Method one used in setting-up the EMCO probe as a two port network

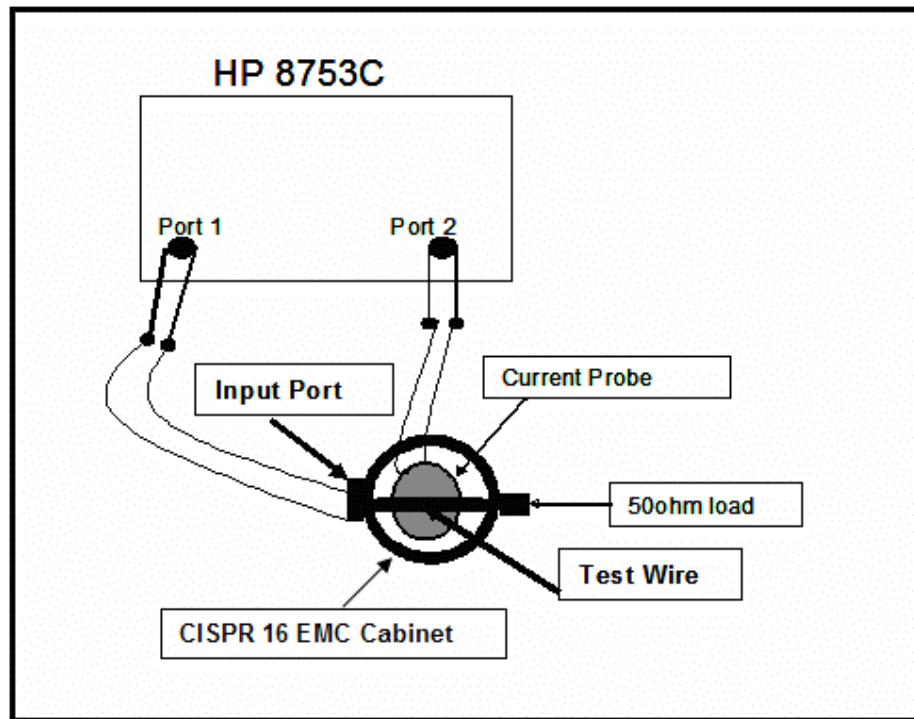


Figure 3-3: Method two used in setting-up the EMCO probe as a two port network

The first verification method used a Vector Network Analyser (VNA) in conjunction with a small rectangular metal container consisting of a copper wire (the conductor) terminated in a 50Ω load. The purpose of this container is to create a test environment that prevents any common mode currents from creeping onto the test wire that might lead to a contaminated measurement. Port one of the VNA was used to insert a signal onto the conductor producing a current. This current formed the input to the two port EMCO probe measurement network. The second port was the output of the EMCO current probe. This output was fed into port two of the VNA, which recorded the full S-parameters of the EMCO probe.

In the case of the second method, Figure 3-3, the small rectangular metal container with the conductor terminated into a 50Ω load, was replaced with a CISPR 16 metal container. This CISPR 16 structure consisted of a centre conductor where the ratio of the diameter of the conductor to the cavity itself (Figure 3-4 below), constitutes a 50Ω environment. The container provides a screened 50Ω environment within which the characteristics of the EMCO probe's transfer impedance can be determined. The 50Ω environment is due to the fact that the cavity was modelled on a coaxial line with a characteristic impedance of 50Ω as per the equation 3.1 [1] below:

$$Z_o = \sqrt{\frac{\mu}{\epsilon}} \left(\frac{\ln \frac{b}{a}}{2\pi} \right), \quad 3.1$$

where,

$$\mu = 4\pi \times 10^{-7} \text{ H/m [2]} \quad 3.2$$

$$\epsilon = 8.854 \times 10^{-12} \text{ F/m [2]} \quad 3.3$$

'a' and 'b' is indicated in Figure 3-4 below.

Figure 3-4 below depicts the CISPR 16 metal cabinet with the dimensions of the two related inner radiuses 'a' and 'b'.

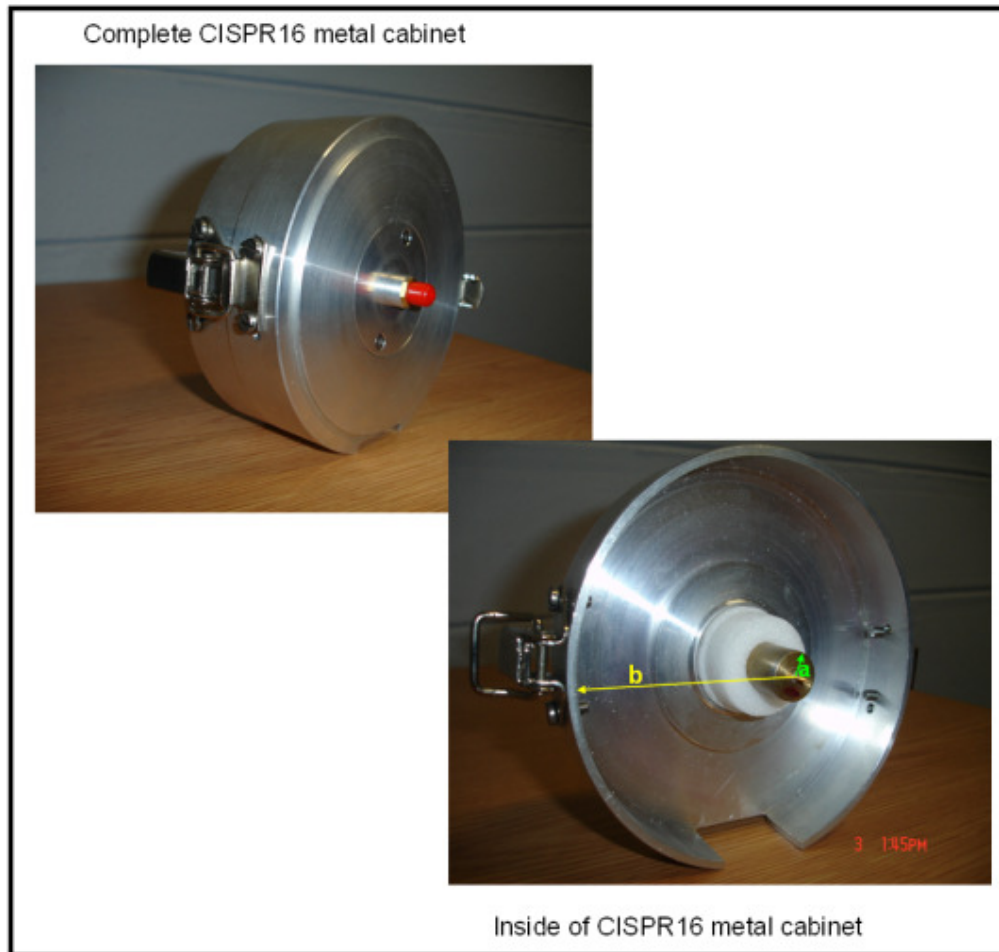


Figure 3-4: Pictures of the constructed CISPR16 metal cabinet used. The lower picture shows the open cabinet for clarity.

For both methods above the same process was followed to extract the required EMCO probe transfer impedance data. The detail on the conversion of the S-parameters to Z-parameters and the calculation of the EMCO probe's Z_t is captured in Appendix D as part of the Matlab code that was written to ultimately compare the measured Z_t with the supplied Z_t (see Figure 3-5).

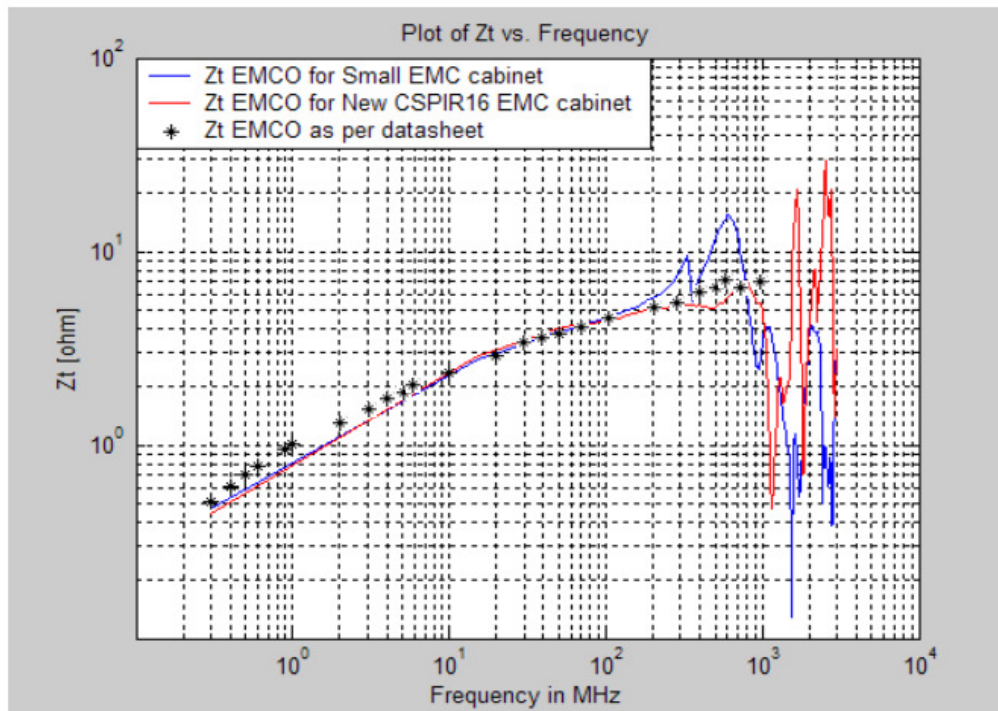


Figure 3-5: A comparison between the measured and supplier provided EMCO probe transfer impedance data

3.3 Discussion of the verification results

The purpose of the verification process was to confirm the provided transfer impedance data. Two verification techniques (Figure 3-2 & Figure 3-3) were used. The results of these two methods are captured in Figure 3-5, from which the following can be extracted:

In the case of the Small EMC cabinet a resonance at 600MHz is visible. The reason for the resonance is primarily due to length of the return path of the signal that constitutes a frequency related standing wave. This was confirmed by investigating the effect of the possible current paths within the cabinet. The results of this investigation are captured in Figure 3-6 below.

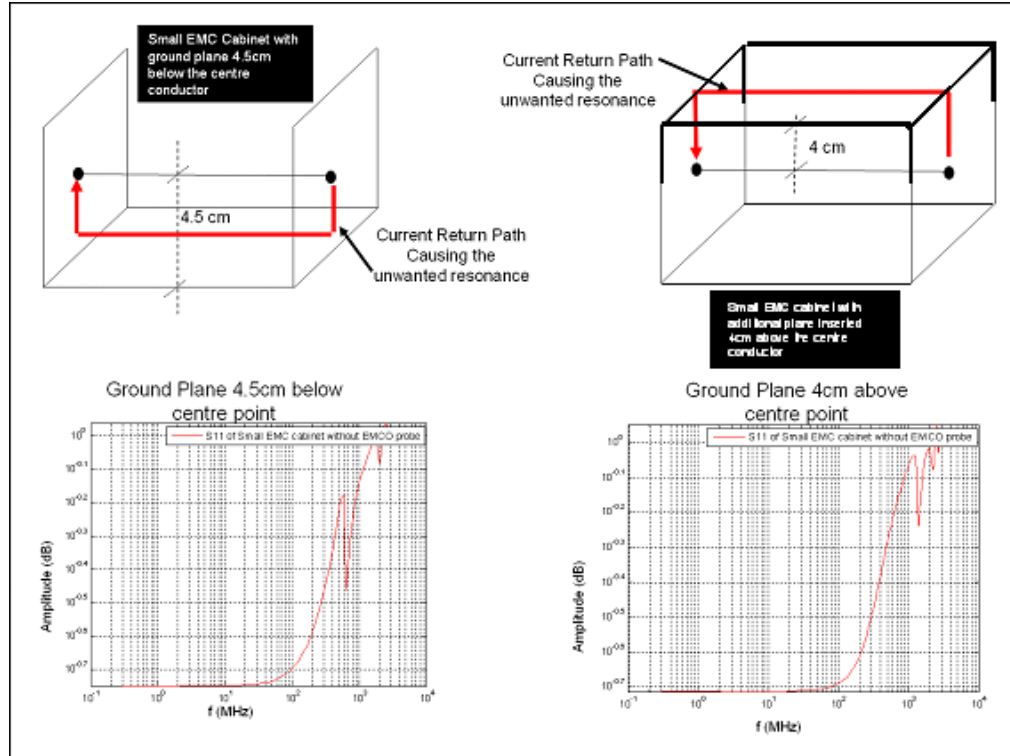


Figure 3-6 Schematic of the test set-up and related results linked to the investigation on the unwanted resonance with the small EMC cabinet used to calibrate the EMCO probe

As seen in Figure 3-6 above, the cabinet as an entity on its own was evaluated. The focus was to establish whether the unwanted resonance that occurred during the verification process was due to either the capacitive coupling between the EMCO probe and the cabinet or due to the physical construction characteristics of the cabinet itself. Note that this unwanted resonance only occurred whilst using the small EMC cabinet and not the CSIPR 16 cabinet. Hence the reason that the investigation into the root causes of the unwanted resonance is only directed towards the small EMC cabinet. The focus of the investigation was to establish whether the cabinet constitutes a resonance or not

In Figure 3-6 the test set-up for the investigation of the EMC cabinet is displayed. The following test methodology were executed:

- a. A network analyser was connected at the input of the cabinet and a 50Ω load at the opposite side
- b. The VNA was used to measure the S11 characteristics of the cabinet.
- c. These results were plotted using Matlab (see Figure 3-6).
- d. The results were evaluated to establish whether the cabinet itself has the same S11 behaviour as in the case of the EMCO probe transfer verification tests.

After commencing the investigation following the above listed steps, it was found that the cabinet itself contains a resonance at 600 MHz. This was confirmed as follow:

- a. Measuring the return path, which was 37.5cm
- b. Multiplying the measured distance of the return path with the calculated speed at which the signal travels, which produced a time value of 1.67 ns. This time value equated to an equivalent frequency value of 600 MHz, which is the exact value of the unwanted resonance.

After discovering the above relation between the return path of the supplied signal and the unwanted resonance within the cabinet, steps were taken to 'move' the resonance beyond the 1 GHz frequency point, which is the upper limit of the frequency band of the EMCO probe. Knowing the theoretical relationship between the distance of a return path and the consequent resonance frequency, it was calculated that the distance of the required return path should be 18.7cm. The only practical way to obtain the required distance was to place the ground plane 4cm above the centre conductor of the cabinet. This resulted in a resonance frequency equivalent to 1.2 GHz as per the predicted theory. This result confirmed the theoretical correlation between the return path and the resonance frequency associated with the EMC cabinet. However, due to the space limitation introduced by the addition of the base-plate, it prohibited the use the cabinet for its intended purpose within the spectrum of this investigation. Therefore method one did

not succeed in verifying the transfer impedance data. As opposed to the Small EMC cabinet, the new CISPR16 metal container showed no unwanted resonances within the desired frequency band. Thus, method two was successful in confirming the transfer impedance data of the EMCO probe. Finally, because the transfer impedance data of the EMCO probe has been confirmed, the EMCO probe was deemed fit to be used as the primary BCI equipment for the equivalence tests captured in chapter 5.

3.4 References

- [1] David M. Pozar, *Microwave Engineering 2nd Edition*, Page 65, John Wiley & Sons, Inc.
- [2] David M. Pozar, *Microwave Engineering 2nd Edition*, Page 704, John Wiley & Sons, Inc.

4 Modified TEM Cell

4.1 Introduction

In testing for the electromagnetic immunity of electrical and electronic devices, various tests and test equipment are used. The tests and related equipment are a function of the test standard against which the equipment is tested.

One of the important aspects of immunity tests is the repeatability. The conventional method used to perform these test is to illuminate the DUT with an electromagnetic wave using an antenna in its the far field. This establishes a uniform electromagnetic wave, which primarily contributes towards repeatable tests. The TEM cell is a device that can also generate a uniform TEM field within a constructed environment [1]. Therefore, in the context of this work the TEM cell qualifies as an in-house option to perform these repeatable immunity tests. However, a conventional TEM cell has certain requirements for construction that complicate it as a simple in-house device. Therefore a decision was made to design a modified TEM cell with

an operational bandwidth of 0Hz to 500MHz. This frequency band is biased by the industry specific required test frequencies, namely a fundamental of 50MHz plus the related harmonics up to the 9th. However, although the desired bandwidth is only till 500MHz, the modified TEM cell was characterised up to 3GHz to study its performance in the higher bands. The difference between modified TEM cell versus the original TEM cell constructed by Crawford can be summarised as follows:

- a. The TEM cell designed by Crawford is based on a rectangular coaxial structure.
- b. The modified TEM cell is essentially an expanded microstripline with an air dielectric substrate.

In the following subsections, the detail design of the modified TEM cell is presented.

4.2 Theoretical Design of the modified TEM Cell

In the following two sub-sections attention is given to the detail design of the two principle parts of the modified TEM cell:

- a. The taper or feed area
- b. The uniform area

The subsequent subsections will discuss the detail pertaining to the design of these two areas.

4.2.1 Taper Design

As noted in Figure 4-2 below the modified TEM cell consists of a taper and a uniform area. Due to the physical size difference between these two areas, there is also an impedance difference or mismatch between them. The primary function of the taper is to prevent or minimise signal loss between these two areas due to the impedance mismatch. Various tapers exist, for example the Klopfenstein, Triangular and Exponential. To choose a taper, the size constraints and performance within the frequency band are some of the typical parameters to consider. For this investigation the exponential taper was chosen mainly due to its performance in the frequency band of interest ($BL \leq \pi$) compared to the other two options as per [6]. To calculate the S11 of the exponential taper the following formula [3] was used:

$$|\Gamma(\varphi)| = \frac{1}{2} \left(\frac{ZL}{Z_0} \right) \left[\frac{\sin(BL)}{BL} \right], \quad 4.2$$

Where,

$|\Gamma(\varphi)|$ is the absolute value of the reflection coefficient of the taper, ZL is the load impedance of the TEM cell, Z_0 is the characteristic impedance of the TEM cell's uniform area, L is the length in metre of the taper and B is the

propagation constant. A graphical representation of the magnitude of the S_{11} of the exponential function is depicted in Figure 4-1 below. The length of the taper is 0.3m (a length chosen in relation to anticipated final product size), the load impedance is 50Ω and the characteristic impedance is 100Ω . The uniform area effectively represents a parallel plate structure. As per [7] the characteristic impedance of a parallel plate structure is defined as:

$$Z_0 = \eta d/W, \quad 4.1$$

Where,

η = Intrinsic impedance of the medium between the two plates which is that of free space, namely 377Ω [8]; d is the distance between the plates and W the width of the bottom plate, which is effectively the ground plane of the TEM cell. The physical width of the TEM cell's ground plane is 500mm, however operationally the TEM cell is used within a RF chamber where it is placed on the ground plane of the chamber. Therefore the effective ground plane of the TEM cell is that of the RF chamber which is approximately three times that of the distance between the top plate and the ground plane of the uniform area. Therefore replacing the parameters of equation 4.1 with the actual values produces a characteristic impedance of 100Ω .

The Figure 4-1 was generated using a Matlab software programme (Appendix A).

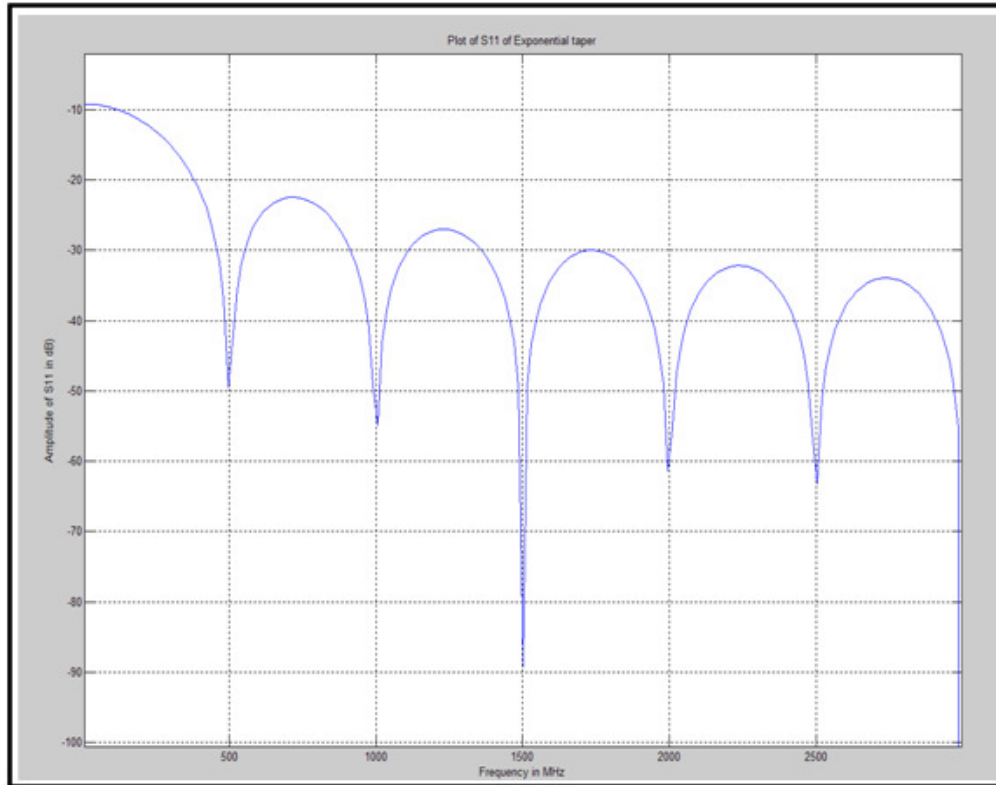


Figure 4-1: Graphical representation of the S11 of the exponential taper as per equation 3.1 above

From Figure 4-1 the following information can be extracted, namely: The optimal operational frequency band of the taper occurs after 500MHz, which is in contrast with the desired bandwidth. However, below 500MHz the maximum reflection coefficient is equal to -10dB, which equates to a loss in power of 10 percent. Therefore, although the length of the taper (300mm) constitutes to an effective taper bandwidth of 500MHz, the compromise of 10 percent of the input power versus the practical desired geometric requirements is deemed as acceptable.

The next step in the design of the taper is to calculate the physical dimension of the taper, namely the width and height. This data is used to physically construct the taper. Figure 4-2 below provides a graphical representation of the widths and heights of the taper.

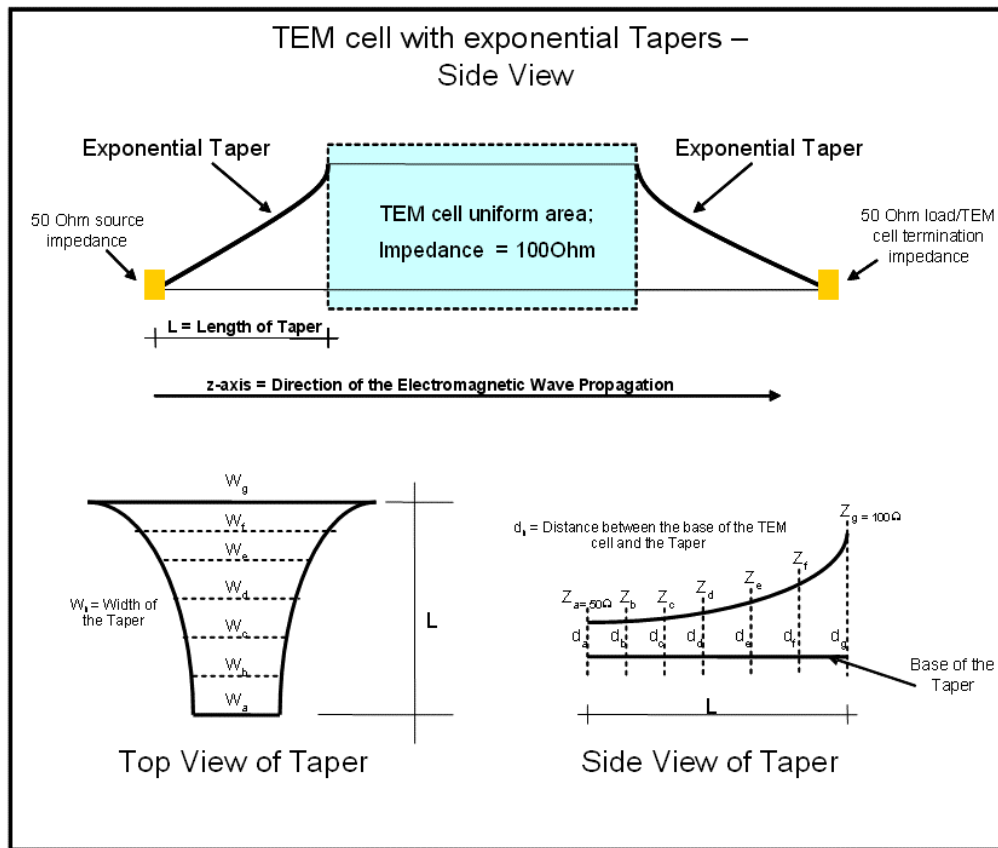


Figure 4-2: A graphical representation of the exponential tapers of the TEM cell

The following process was followed to calculate width and height dimensions of the exponential taper:

- a. Calculate the impedance of the taper at various distances along the z-axis (as depicted in Figure 4-2 using the following formula [3]:

$$Z(z) = Z_0 e^{az} \quad 4.3$$

where,

Z_0 = The source impedance OR the impedance at $z = 0$

$$a = \frac{1}{L} \ln \left(\frac{Z_L}{Z_0} \right) \quad 4.4$$

$0 < z < L$, where L = the length of the taper along the z-axis

- b. Use the impedance values calculated to determine the width and height of the Taper at the corresponding distances along the z-axis, using the following microstripline formulas [2]:

$$\frac{W}{d} = \frac{8e^A}{e^{2A} - 2} \quad \text{for} \quad \frac{W}{d} < 2 \quad 4.5$$

where,

W = width of the taper (as per Figure 4-2)

d = distance between the base of the TEM cell and the taper (as per Figure 4-2)

$$A = \frac{Z_0}{60} \sqrt{\frac{E_r + 1}{2} + \frac{E_r - 1}{E_r + 1} \left(0.23 + \frac{0.11}{E_r} \right)} \quad 4.6$$

where,

$E_r \sim 1$, (Relative permittivity of air)

thus,

$$A = \frac{Z_0}{60} \quad 4.7$$

After implementing the taper design methodology, the calculated values for the identified design parameters of the exponential taper are summarised in Table 4-1 below.

Table 4-1: Table summarising the width and height dimensions of the exponential taper

z value (distance from source mm)	Calculated Width [W(mm)]	Chosen height [d(mm)]	Calculated Impedance [Z(z) Ohm]
9	12	3	50
18	52	10	51
27	76	15	52
36	92	22	53
45	128	29	54
54	157	35	56
63	180	43	57
72	204	50	58
81	228	58	59
90	245	65	60
99	260	70	62
108	284	80	63
117	300	87	64
126	323	97	66
135	342	107	67
144	358	116	69
153	371	125	70
162	384	134	71
171	400	140	73
180	412	154	75
189	423	164	76
198	436	174	78
207	446	182	79
216	457	196	81
225	468	208	83
234	480	222	85
243	486	235	86
252	486	248	88
261	486	260	90
270	486	271	92
279	486	284	94
288	486	295	96
297	486	333	98
306	500	335	100

4.2.2 Design of the Uniform Area

The second important part of the modified TEM cell is the uniform area. The uniform area is the area where a uniform electromagnetic wave is present, hence the area where the DUT will be situated. The width and the height of this area is equal to the maximum width and height dimensions of the taper as captured in Table 4-1 above. Within the uniform area the E-field component of the present electromagnetic wave is the component of interest. To calculate the generated E-field to be found in the uniform area, the area is seen as a parallel plate and the following equation is used:

$$E = \frac{V}{d} \quad 4.8$$

where,

E is the E-field, V is the voltage in that region and d is the height dimension of the area.

Another important aspect to know about the uniform area of the TEM cell is the bandwidth. However, prior to calculating the bandwidth of the area a brief discussion on modes will commence. This is done, because modes have a direct impact on the bandwidth.

There are three types of modes, namely Transverse Electric (TE), Transverse Magnetic (TM) and lastly Transverse Electric and Magnetic (TEM). The TEM mode is the fundamental mode that can exist at all frequencies. This effectively means that if a uniform electromagnetic field is generated within a cavity that retains a TEM mode characteristic, the bandwidth of the system is infinite. However due to the physical dimension of a cavity higher order TE and TM modes will be present beyond their cut-in frequencies. These higher order modes are also the determining factors that limit the bandwidth of a TEM mode.

Figure 4-3 below depicts the TEM cell with its physical dimensions.

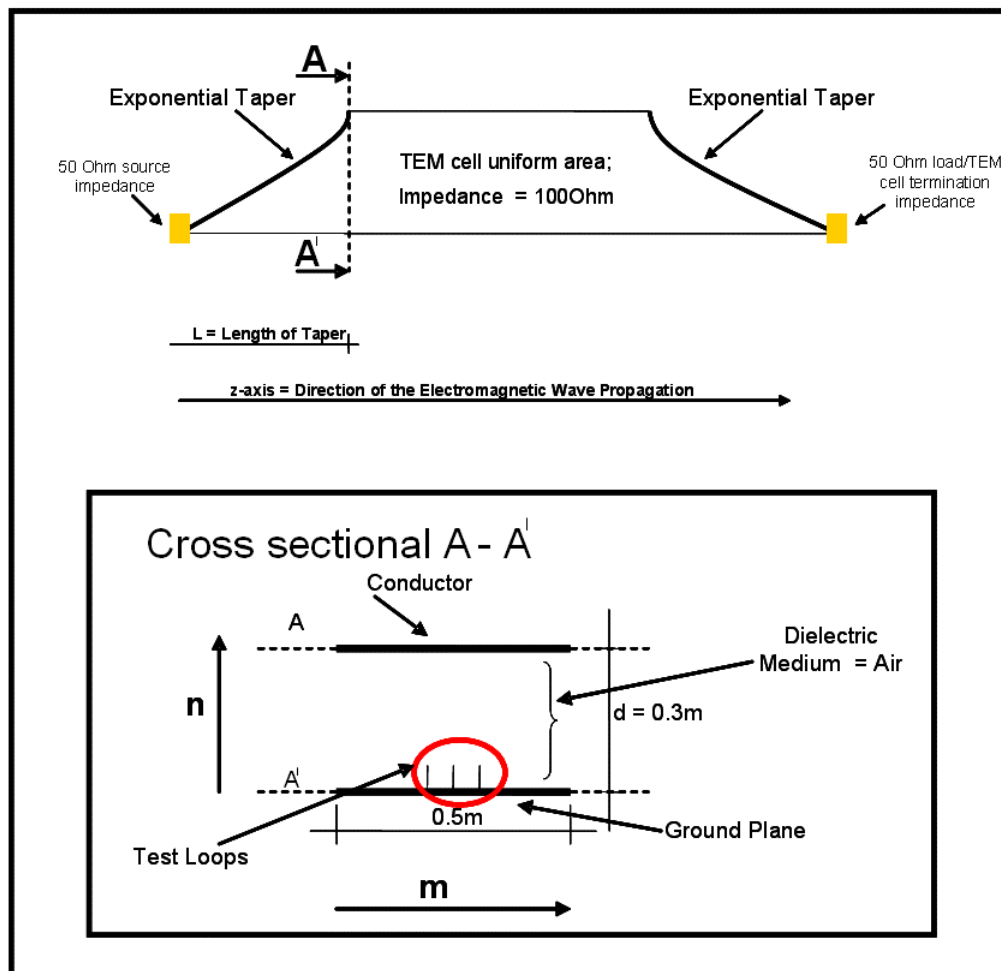


Figure 4-3: A cross sectional view of the TEM cell identifying the dimensions of the TEM cell that are parameters of the higher order modes of the parallel-plate related cavity or wave guide

Note that the test loops indicated in Figure 4-3 above were inserted to simulate the device under test. These loops also play an integral part of the equivalence testing procedure described in detail in subsequent sections. Note, the height of the device under test cannot be too great or it will distort the uniformity of the fields in the TEM cell. This has been chosen not to exceed a third of the height of the cell for geometrical reasons. The literature, e.g. [9] agrees with this basic point. The height of the loops must then be less than 10cm. Although the TEM cell is not an exact replica of the reference structure in [9], the relationship between the height of the device under test compared to the height of the TEM cell was used as a guideline. In a latter section of the thesis the uniformity of the uniform area in TEM is

investigated, the rational in terms of confirming whether or not the mentioned guideline used was effective or not, was that if the uniformity test reveals uniformity discrepancies greater than 3dB, then one of the parameters that will change is the chosen height of the test loops. However if it is not the case the guideline is deemed as sufficient. To calculate the bandwidth of the TEM cell, the cut-off frequencies related to the various higher order modes need to be calculated. To calculate the cut-off frequencies of the dominant higher order modes the following equation was used [4]:

$$f_c = \frac{nc}{2d} \quad 4.9$$

where,

n = the number of the mode or the number of half-wavelengths between plates

c = speed of light

d = distance between the ground plane and the conductor (dielectric (Air))

Table 4-2: Summary on the calculated values of the cut-off frequencies of the higher order TE and TM modes in the TEM cell

Mode number (n)	Cut-off frequency (f_c) (MHz)
1	500
2	1000
3	1500
4	2000

Based on the values as per Table 4-2 the bandwidth of the TEM cell stretches from 0 Hz to 500 MHz, after which the higher-order modes associated with the physical dimensions of the TEM cell start to manifest. For all practical reasons this means that between 0Hz and 500MHz a uniform E-field can exist within the uniform area of the TEM cell.

Thus to summarise the theoretical design of the TEM cell:

1. Firstly a decision was made to base the design a modified TEM cell instead of the conventional Crawford model. The rationale behind the decision was primarily to keep the construction of the TEM cell as simple and cheap as possible, seeing that it must be used as an in-house built device.
2. Secondly the taper of the TEM cell was designed. From that process the following information were generated:
 - i. A graphical representation of the magnitude of the S11 of the taper revealing that between 0Hz to 500MHz a maximum reflection coefficient of -10dB is measured, which equates to a loss in power of approximately 10 percent.
 - ii. The width and related height dimensions were calculated. These data act as the input for the physical construction of the taper.
3. Thirdly the uniform area was designed. Here the following information was extracted:
 - i. The width and height dimensions are equal to the maximum width and height dimensions of the taper as per design preferences.
 - ii. The height dimension also plays a critical role in determining the field strength of the desired E-field.
 - iii. The bandwidth of the uniform area was calculated taking into consideration the effect of the higher order TE and TM modes, which is caused by the physical dimensions of the uniform area.

4.3 Practical Construction of the Modified TEM Cell

The construction of the TEM cell was guided by the calculated values as per Table 4-1. However, special attention was given to the taper area of the TEM, namely, slots were introduced on top of the taper area (see Figure 4-4). The fundamental theory on modes stipulates that the transverse dimension should be less than half of the related wavelength to prevent the next higher order mode from cutting in. For the constructed TEM cell the maximum distance between the ground plane and the taper is 300mm, which satisfy the half wavelength criteria for a higher mode to exists (which is TE₀₁ at 500MHz as indicated in Table 4-2). Therefore, by inserting the slots the induced currents should be prohibited to flow, hence eradicating the effect of the higher order mode within the taper area. However, explicit measurements were not performed to confirm the theory. Instead, a decision was made to monitor the uniformity test results presented in a latter stage in this document, and based on that, make a call on whether or not further effort should be committed towards ensuring the eradication of the higher order modes effects within the taper area. It can be stated that the results revealed that within the desired bandwidth acceptable uniformity levels exists, hence no further attention to the slots were given. To conclude this point, the author does wish to highlight the fact, that for further work in this regard, detail characterisation and validation of the slots and its contribution towards the eradication of unwanted higher order modes within the taper area, will enhance the current work performed.

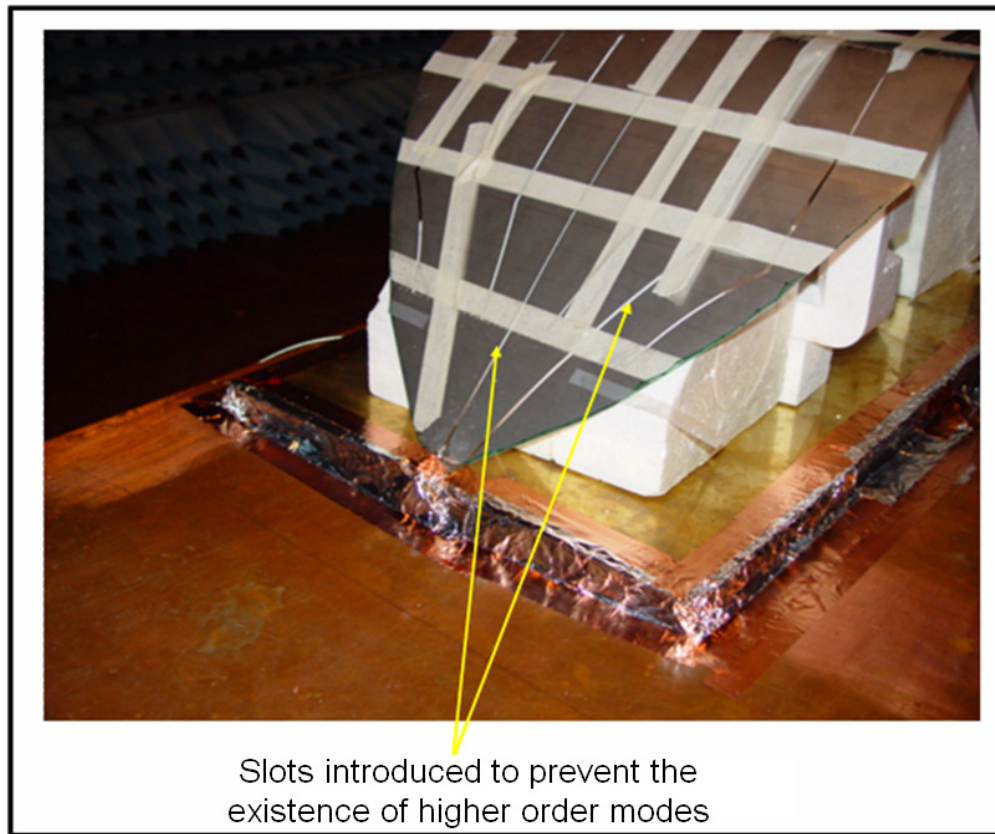


Figure 4-4: An illustration of the slots on top of the Taper part of the TEM cell

Within the uniform area three test loops were inserted as well as a special constructed uniformity test plate (Figure 4-5 below) to perform the required uniformity tests. The detail on how the test loops were incorporated into the equivalence testing is covered in subsequent sections.

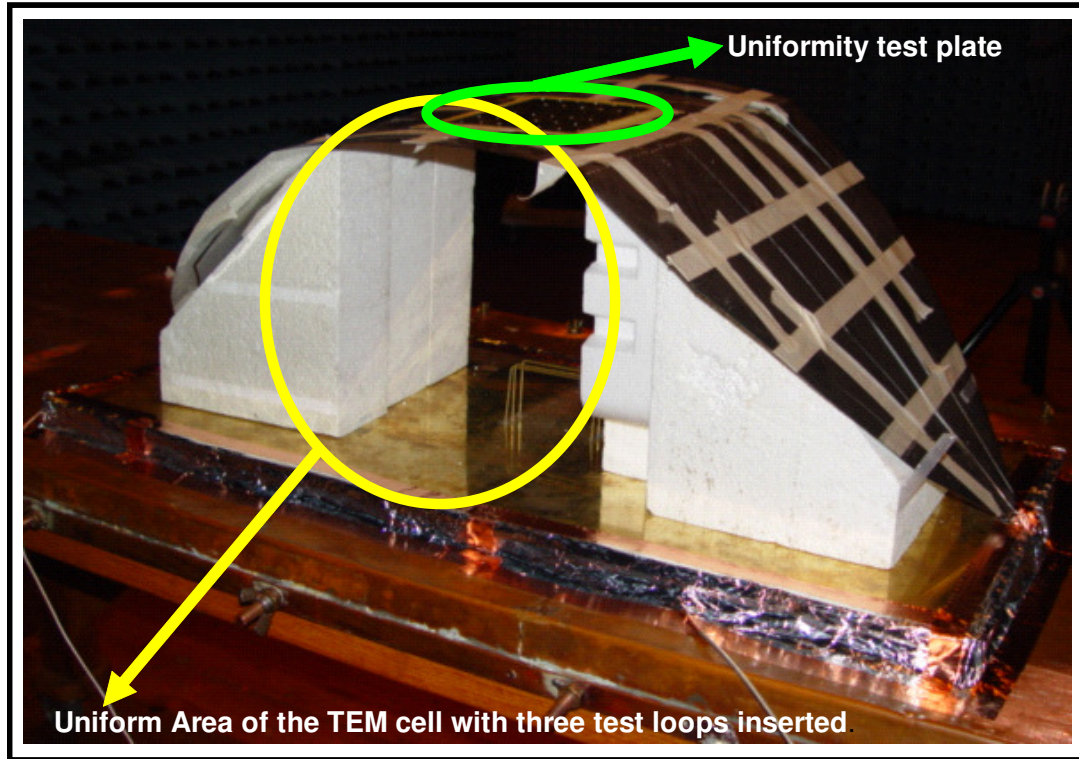


Figure 4-5: The uniform area of the constructed Tem cell with the three test loops and uniformity test plate

4.4 Test and Evaluation of the modified TEM cell

The TEM Cell has two characteristics that were evaluated:

- The taper
- The uniformity of the TEM Cell within the area of interest

4.4.1 Evaluating the Modified TEM cell taper effectiveness

The function of the taper is to reduce loss of the input signal between the points where the signal is inserted into the Tem Cell and the uniform region of TEM Cell. The taper was designed to gradually increase the initial impedance experienced by the input signal, from 50 Ohm to 100 Ohm, which is the characteristic impedance of the uniform region of the TEM Cell.

4.4.1.1 Test Methodology and Measurement Results

To establish the correlation between the theoretical and measured S11 of the taper the measurement set-up of Figure 4-6 below was constructed. These results are presented in Figure 4-7.

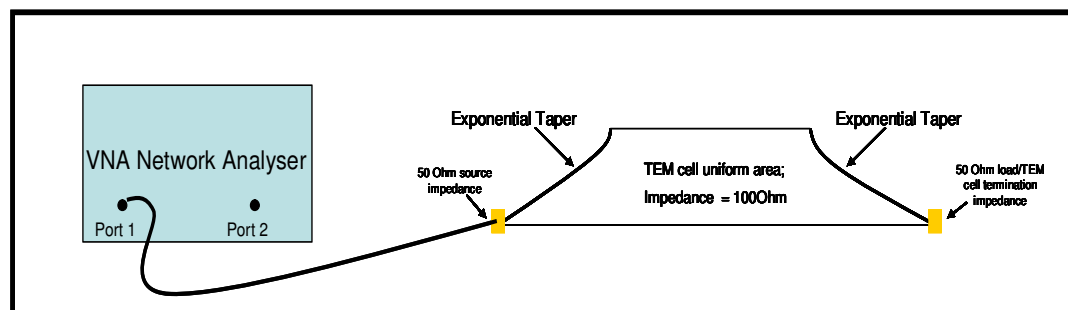


Figure 4-6: Measurement set-up used to execute the TEM cell taper S11 measurement

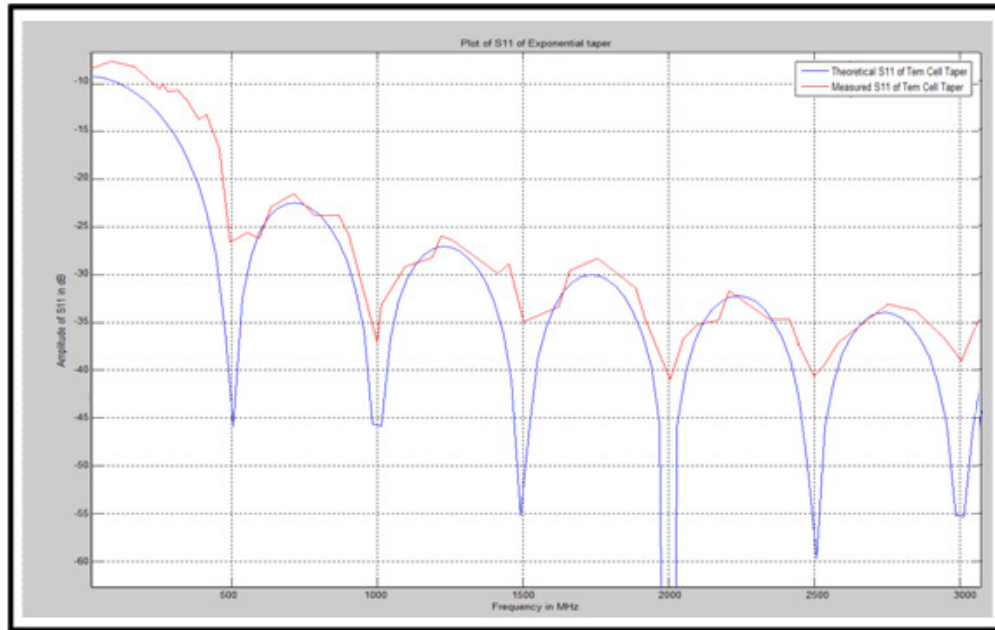


Figure 4-7: Reflection coefficient measurement results of the constructed TEM Cell

4.4.1.2 Discussion of results

The important aspect of the S11 measurement in the context of the TEM cell design is the fact that it provides information on the percentage of power loss that will occur due to the taper. From Figure 4-7 it is evident that the measurement confirmed the theoretical prediction.

4.4.2 Evaluating the Uniformity of the Modified TEM Cell

The following subsections describe in detail the test methodology, results obtained and a discussion on the related results.

4.4.2.1 Test Methodology and Results

The purpose of this test was to establish the E-field uniformity of the TEM cell within a specific region of interest. To capture the data a S21 measurement was performed on the TEM cell using a Vector Network Analyser (VNA) in conjunction with an E-field probe as per Figure 4-8. The results obtained from the S21 measurement performed were fed into a Matlab software programme (Appendix C) to generate contour plots of the E-field distribution. Note that the E-field probe was used to measure the E-field within the uniform area of the TEM from on top of the cell through the special constructed matrix structured plate with holes. It would have been beneficial to measure the E-field at various heights in the TEM cell, however this measurement had the risk of interference with the existing E-field, hence contaminating the integrity of the measurement.

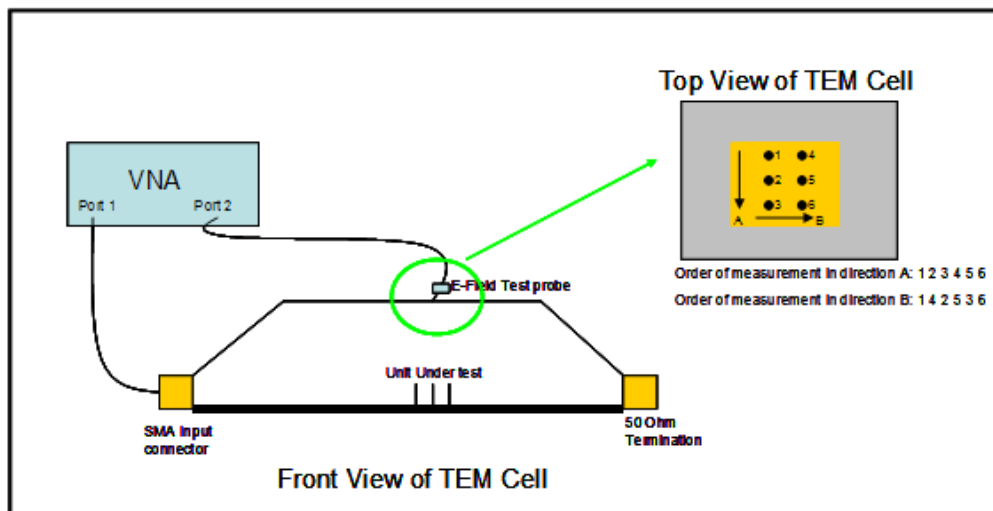


Figure 4-8: The test set-up for the uniformity tests performed on the TEM cell

The results obtained from the uniformity tests are displayed in Figure 4-9 below.

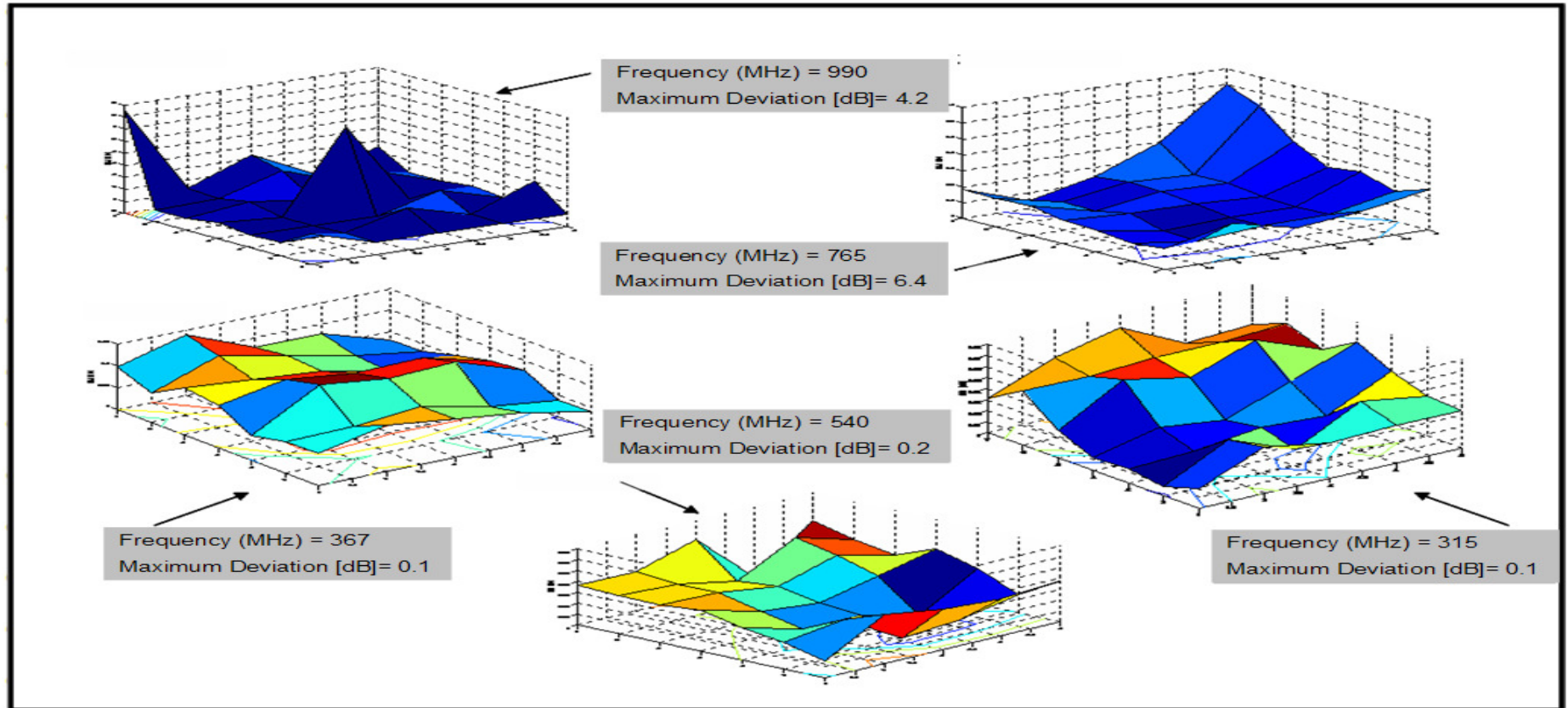


Figure 4-9: Results obtained from the TEM cell uniformity measurements

4.4.2.2 Discussion

Figure 4-9 attempts to provide a graphical representation of the uniformity measurements at the related frequencies. In presenting a global overview of the results some of the picture resolution were compromised. However the value adding information is extracted and presented in Table 4-3 below, focusing on the critical measurement parameters, namely: test frequency and the maximum deviation.

Table 4-3: Summary of TEM cell uniformity measurements

Test Frequency (MHz)	Maximum Deviation (dB)
990	4.2
765	6.4
540	0.2
367	0.1
315	0.1

The measurements were explicitly performed within the bandwidth frequencies of the TEM, with the exemption of two, namely 765MHz and 990MHz. This was done to investigate the uniformity both within and outside the calculated bandwidth (0MHz to 500MHz) of the TEM cell. Based on the results as per Table 4-3 it is evident that within the calculated bandwidth of the TEM cell the maximum deviation measured is 0.1dB. However outside the bandwidth a maximum deviation of 6.4dB was measured. Hence it can be stated that within the bandwidth of the TEM cell the measurements confirmed uniformity with a maximum variation of 2 percent. Note, the author do wish to state that using more frequency points within the desired bandwidth will provide a higher level of statistical confidence in terms of the results obtained.

4.5 Conclusion

This chapter focused on the design, construction and evaluation of a TEM cell. The TEM cell was originally known as a Crawford cell as he was the individual who first designed it. Effectively a TEM cell is a device that has the ability to generate a uniform E-field within a specified area of interest. The complexity linked with the construction of the Crawford version of a TEM cell led to the decision to construct a modified TEM cell based on a microstripline with an air dielectric substrate.

The design of the TEM cell is comprised of two phases, namely the design of the taper and the uniform area. Within the context of the TEM cell the function of the taper is to ensure a minimal power loss. This was investigated by comparing the theoretically calculated S_{11} with the practically measured S_{11} . The results revealed the taper will impose a maximum return loss in the close vicinity of -10dB (or a 10 percent loss in power) between 0MHz to 500MHz (see Figure 4-7). This percentile was found to be acceptable in the context of the equivalence measurements yet to be performed. The critical aspect in terms of the uniformity region was to calculate the bandwidth of the TEM cell. This was done by calculating the cut-off frequencies of the higher order TE modes (which is a function of the physical dimensions of the TEM). This resulted in a bandwidth that stretches from 0MHz to 500MHz as captured in Table 4-2. After constructing the Tem cell the uniformity of TEM cell was confirmed within the calculated bandwidth of the TEM cell (see Table 4-3).

4.6 References

- [1] M.L. Crawford, "Generation of Standard EM Fields Using TEM Transmission Cells", IEEE Trans. On Electromagnetic Compatibility, Vol. EMC-16, No.4, p189, 1974
- [2] David M. Pozar, *Microwave Engineering 2nd Edition*, Page 160, John Wiley & Sons, Inc.
- [3] David M. Pozar, *Microwave Engineering 2nd Edition*, Page 290, John Wiley & Sons, Inc.
- [4] David M. Pozar, *Microwave Engineering 2nd Edition*, Page 118, John Wiley & Sons, Inc.
- [5] K. Malaric, J. Bartolic, "Design of a TEM-Cell with increased usable test area", Turk J Elec Engin, Vol.11, No.2, 2003
- [6] David M. Pozar, *Microwave Engineering 2nd Edition*, Page 294, John Wiley & Sons, Inc.
- [7] David M. Pozar, *Microwave Engineering 2nd Edition*, Page 113, John Wiley & Sons, Inc.
- [8] David M. Pozar, *Microwave Engineering 2nd Edition*, Page 17, John Wiley & Sons, Inc.
- [9] M.L. Crawford, "Generation of Standard EM Fields Using TEM Transmission Cells", IEEE Trans. On Electromagnetic Compatibility, Vol. EMC-16, No.4, p190, 1974

5 Proof of Equivalence

This chapter considers experimental equivalence between in-house and conventional EMC tests.

5.1 Test Methodology

The test methodology used to perform the equivalence tests can be divided into the following phases:

- a. Calibration of the TEM cell
- b. Calibration of the current probe
- c. Proof of Equivalence

The rest of this section will discuss the three phases of the test methodology in detail. However, prior to discussing the three methods of proving equivalence Figure 5-1 below provides a graphical overview of the test methodology.

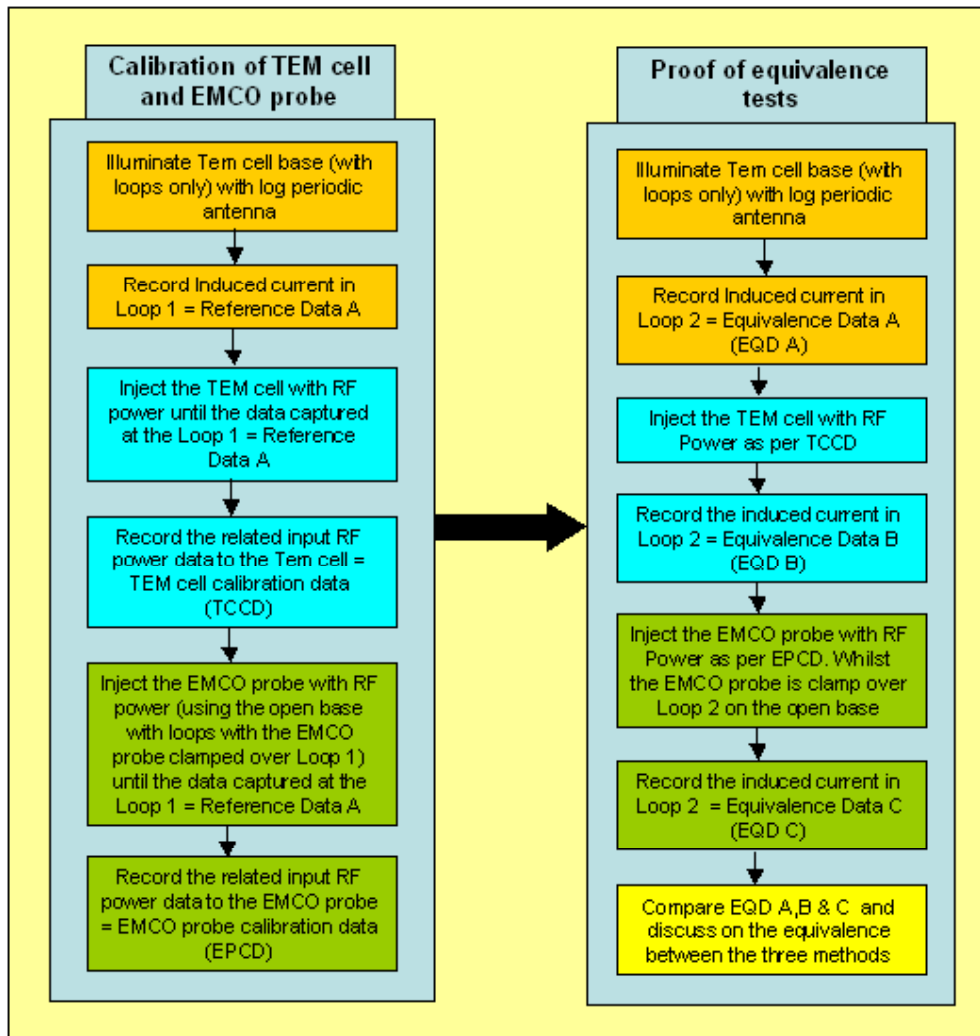


Figure 5-1: Graphic outlay of the complete process followed to prove equivalence between the three EMI measurement techniques

5.1.1 Calibration of the Modified TEM Cell

The calibration process of the modified TEM cell can be divided into two phases, namely the acquisition of the reference calibration data and then the calibration of the modified TEM cell.

5.1.1.1 Acquisition of the Reference Calibration Data

The Houwteq EMC test facility in Grabouw was used to perform all the equivalence related measurements. Therefore, prior to the acquisition of the reference data used as input for the calibration process, the consistency of the Houwteq test set-up (Log-periodic antenna, Holladay probe) was investigated (although the lab confirmed the validity of the test site for the required tests, this exercise it can effectively be viewed as a high-level uncertainty budget investigation). Figure 5-2 illustrates the set-up used to achieve the above stated objective.

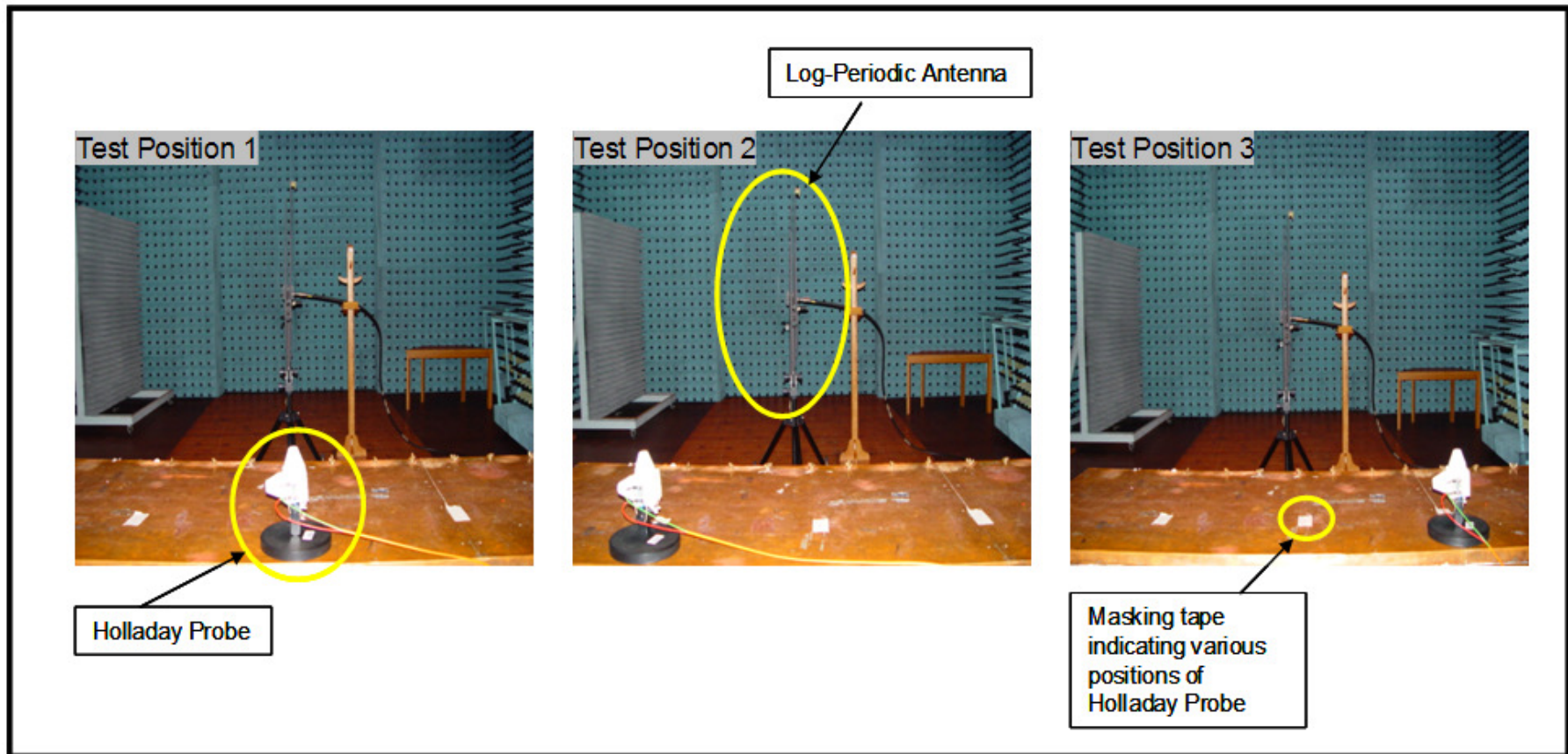


Figure 5-2: The test set-up used to establish the consistency of the generic test set-up probe

The test philosophy used to establish the consistency of the Houwteq generic test set-up can be summarised as follow: Firstly, the log-periodic antenna was used to produce a uniform E-field; secondly, the Holladay probe was placed at three different positions at which a measurement of the E-field generated by the antenna was recorded.. These results are summarised in Table 5-1 below.

Table 5-1: Summary of generic test set-up consistency measurement results

Test Frequency (MHz)	E-field measured at Position 1 (V/m)	E-field measured at Position 2 (V/m)	E-field measured at Position 3 (V/m)
315	5	5.04	5.32

Based on the measurement results summarised in the above table the maximum variation in measurements recorded with the Holladay probe is approximately 0.5dB, which means that the maximum uncertainty level linked to the test results will be in the order of 0.5dB. This variation was deemed to be acceptable in the light of repeatability and integrity of the measurements. After the completion of the Houwteq generic test set-up consistency measurements the collection of the reference data for the calibration of modified TEM cell commenced.

Figure 5-3 below depicts the test set-up used to perform these measurements.

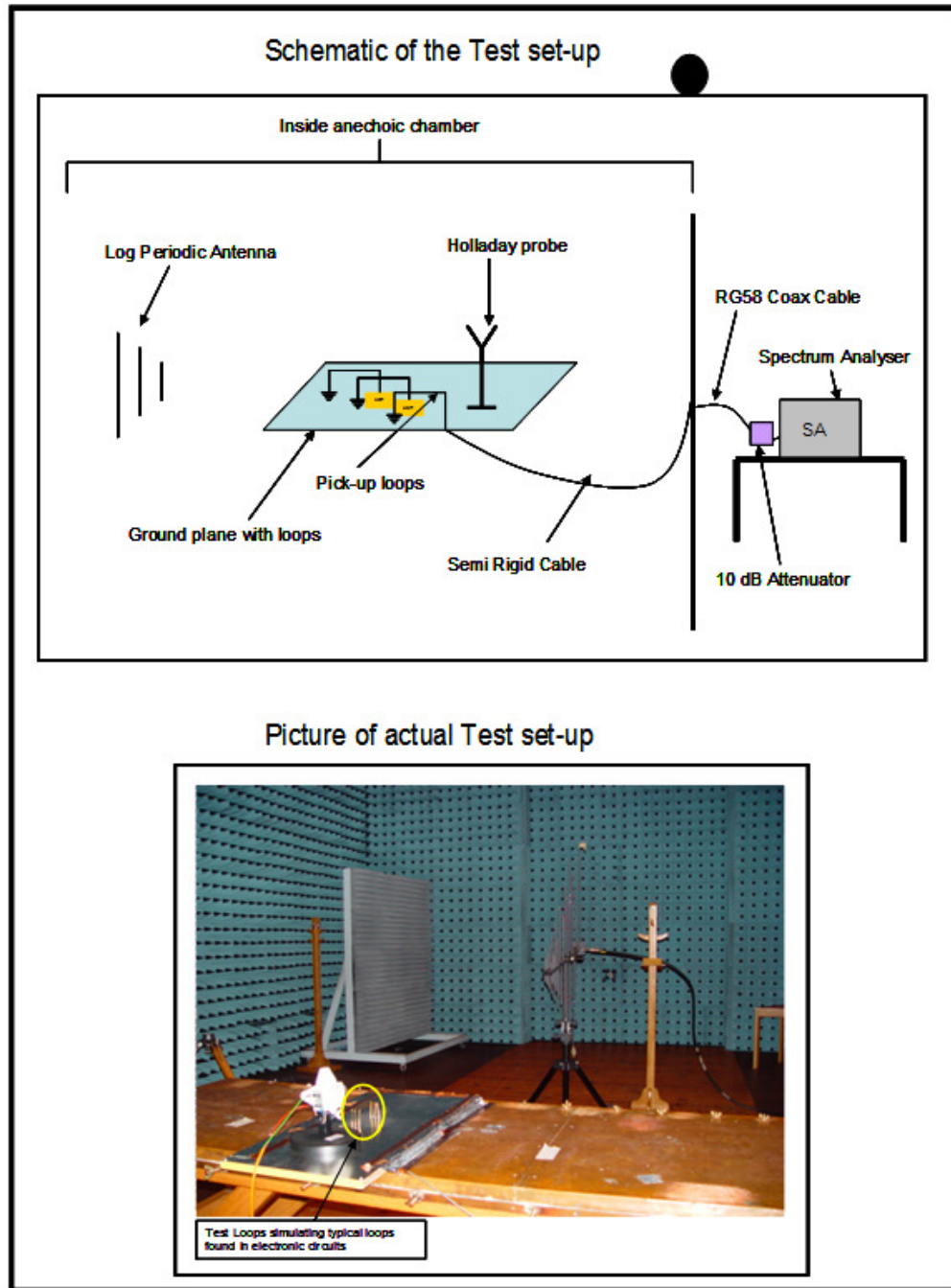


Figure 5-3: Test set-up used to acquire the data is used as the reference data for the calibration of the TEM cell.

To acquire the reference data the following test philosophy was used: 1. The target loops on the open base structure were radiated with an E-field of strength 5V/m (as measured by the Holladay probe); 2. One of the loops was chosen as the target loop. The output of this target loop was the data that was recorded as the reference data, measured in dBuV. The measurement results for the above test are captured in Table 5-2 below.

Table 5-2: A summary of the results recorded that as the reference data for the calibration of the Tem cell

Frequency (MHz)	E-field Intensity (V/m)	Target loop measurement(dBuV)
990	5	81.7
765	5	78.8
540	5	82.8
367	5	84.7
315	5	77.2

The reference data for the calibration in the above table can be interpreted as follow, namely: At a frequency of 315MHz an E-field intensity of 5V/m induces 77.2dBuV in the target loop.

5.1.1.2 Calibration of the TEM Cell

The calibration of the TEM cell is required to ensure that the equivalence measurements performed, as discussed at a latter stage of this document, correlate with the same measurements performed using the log-periodic antenna. This is a correlation specifically in terms of ensuring that the test loops on the open base platform are exposed to the same E-field intensity levels in both instances. Thus, the main focus of the TEM cell calibration process is to establish what the supply RF power to the TEM cell should be (at the various frequencies) to ensure that a uniform E-field is generated in the uniform area of the TEM cell. As noted in Table 5-2 the chosen E-field intensity is 5V/m. This was deliberately done to accommodate the 50Ohm 10W termination resistor used as the load of the TEM cell as depicted in Figure 5-4 below.

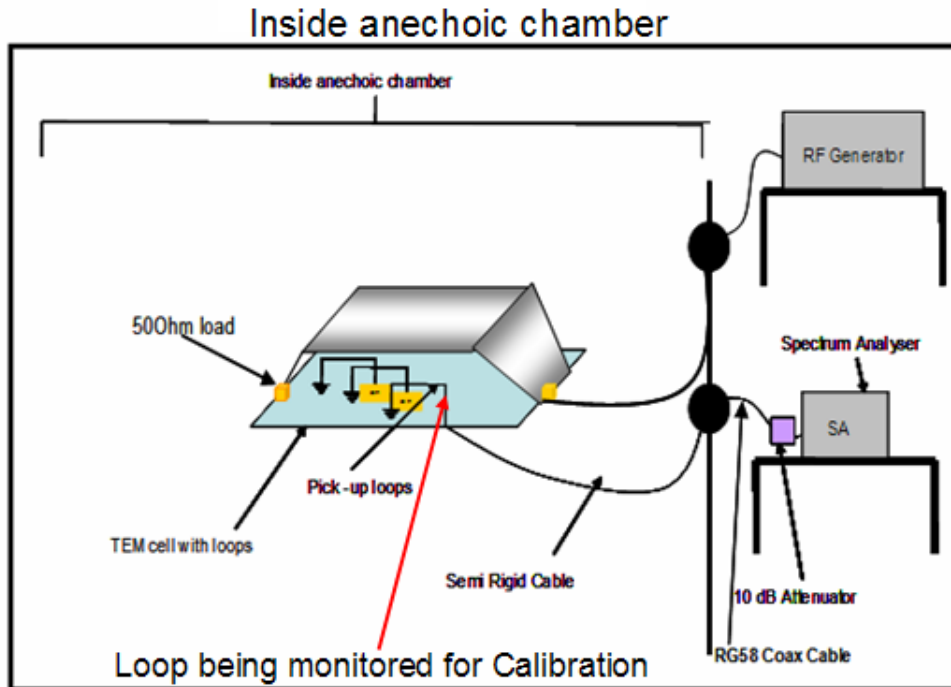


Figure 5-4: Test set-up used to perform the calibration process of the TEM cell

Using Table 5-2 as reference data, the first step in the TEM cell calibration process was to adjust the RF power supplied to the TEM cell until the

current values (in dBuV) as per Table 5-2 in the target loop were achieved. The next step was to record the various input RF power supply values, as these became the calibration values of the TEM cell, meaning that whenever these values of RF power are supplied to the TEM cell (at the various frequencies) an E-field intensity of 5V/m will be present in the uniform area of the TEM cell. These values are captured in Table 5-3 below.

Table 5-3: Input RF power calibration values for the TEM cell

Frequency (MHz)	Supplied RF Power (dBm)	Target loop measurement(dBuV)
990	-36.7	81.7
765	-38	78.8
540	-42	82.8
367	-33.9	84.7
315	-36.7	77.2

The values in Table 5-3 reveal that if the TEM cell is supplied with an input RF power of -33.9dBm at a frequency of 367MHz, it will produce a uniform E-field of 5V/m inducing a current of 84.7dBuV into the target loop within the uniform area of the TEM cell. This information is used in the subsequent sections to evaluate the equivalence between using a TEM cell versus a log-periodic antenna to perform EMC susceptibility tests.

5.1.2 Calibration of the EMCO Current Probe

As part of the calibration process of the TEM cell, the reference data was first generated as per Figure 5-3. In the context of the calibration process of the EMCO probe this data was used as input to the equivalence process.

Figure 5-5 below depicts the test set-up used to calibrate the EMCO probe.

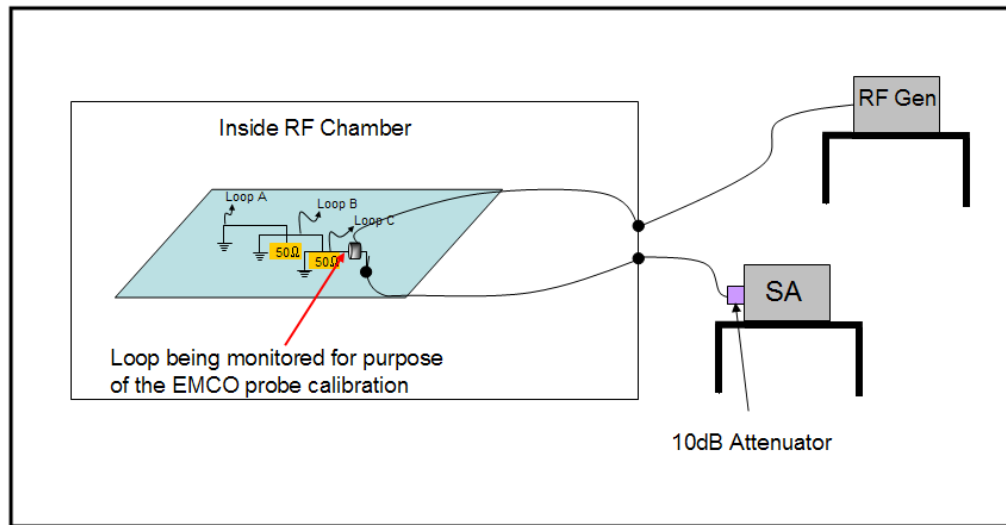


Figure 5-5: Test set-up to capture the calibration data of the EMCO probe

As in the case of the TEM cell, the reason for calibrating the EMCO probe was to ensure that the current injection and radiation method produce an electromagnetic wave within the target loop of similar magnitude. This is critical for ensuring that the equivalence investigation is of high integrity and repeatable.

After the EMCO probe calibration process as per Figure 5-5 above, the following test results were obtained.

Table 5-4: Summary of Calibration data captured for EMCO probe

Frequency (MHz)	Supplied RF Power (dBm)	Target loop measurement (dBuV)
990	10	81.7
765	12	78.8
540	13	82.8
367	13	84.7
315	4	77.2

The primary purpose of the above measurement results was to ensure that the RF power supplied to the test loop via the EMCO probe, equates to an electromagnetic field of strength 5V/m.

5.2 Proof of Equivalence

The purpose of this subsection is to capture the process followed to prove equivalence, record the measurement data and finally to comment on equivalence between the three methods of performing EMC susceptibility tests.

5.2.1 The Process Followed to Proof Equivalence

In the preceding sections both the TEM cell and EMCO probe were calibrated in terms of what input RF power is required at specific frequencies to generate a current equivalent to an E-field with intensity of 5V/m within the test loop of interest. This data was used as input to the following four-fold process used to prove the equivalence between the three test methods:

1. Radiating the loops on the ground plane (using the log-periodic antenna), but monitoring and recording the induced current in a different loop than in the case of the collection of the calibration reference data;
2. Using the TEM cell to expose the loops to a uniform E-field and again (as above) monitoring and recording a different loop than in the case of the calibration process;
3. Injecting the target loop with a current equivalent to 5V/m using the EMCO probe to;
4. Comparing the results obtained in the three above mentioned measurements with the intent of making a conclusive statement on the equivalence between the three methods.

5.2.2 Equivalence Measurements

As explained in the above section, the proof of equivalence entailed three measurements. Figure 5-6 below portrays the test set-up for the measurements performed.

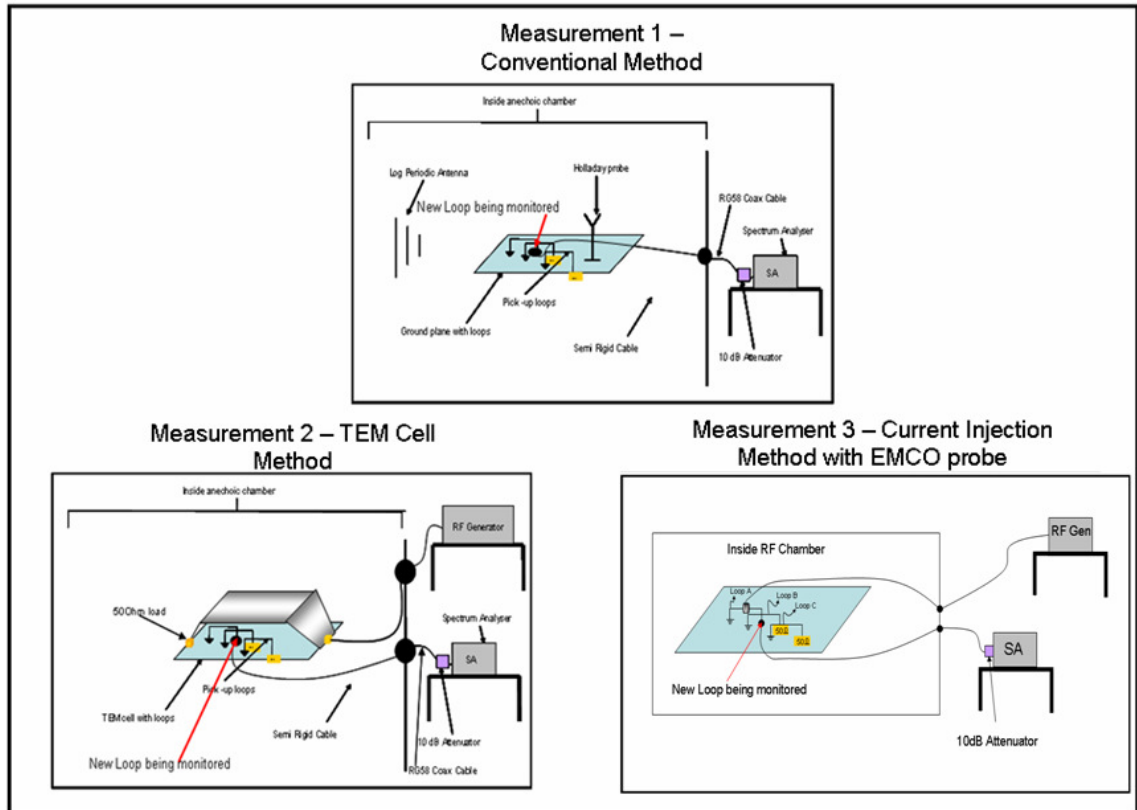


Figure 5-6: The test set-up for the measurements performed to investigate the equivalence between the three EMC test methods

The test results recorded linked to the measurements as per the test set-ups in Figure 5-6 are summarised in Table 5-5 below.

Table 5-5: Measurement results captured for three measurements performed to investigate the equivalence

Frequency (MHz)	Target loop measurement for ground plane loop with log periodic antenna (dBuV)	Target loop measurement with TEM cell (dBuV)	Target loop measurement with EMCO probe (dBuV)
990	81.6	91.2	79.8
765	79.5	87.6	78.8
540	82.7	83.5	81.4
367	84.7	84.3	83.9
315	77.2	78.1	77.8

The discussion on the measurement results captured in Table 5-5 above is presented in the succeeding sub-section.

5.2.3 Discussion on the Equivalence Measurement results

The purpose of this section was to investigate the equivalence between the three EMC susceptibility test methodologies. The intent of the discussion below was to interpret the results captured in Table 5-5 above. The basis of the discussion is a comparison of the results between the Log-Periodic antenna radiation method (LPARM) versus both the TEM cell radiation (TCRM) and EMCO probe current injection methods (EPCIM).

TEM Cell results:

1. Within the bandwidth of the Tem cell (which is from 0Hz to 500MHz) the maximum variation between the measurements performed by the two techniques (LPARM and TCRM) is 0.9dB at a frequency of 315MHz.;
2. Outside the bandwidth of the TEM cell the maximum variation 10.4dB, this significant variation is an example of the effect of higher order modes present in the TEM cell.
3. Based on the measurement data it can be stated that within the bandwidth of the TEM cell equivalence between the LPARM and the TCRM exists within a maximum variation of 0.9dB.

EMCO probe results:

1. Comparing the LPARM with that of the EPCIM results a maximum difference of 0.8dB at 367MHz is observed.
2. Therefore based on the measurements it is evident that equivalence between the two techniques does exist with a maximum variation of 0.8dB.

Within Figure 5-7 below it graphic comparison between the measurement results of three methods is presented.

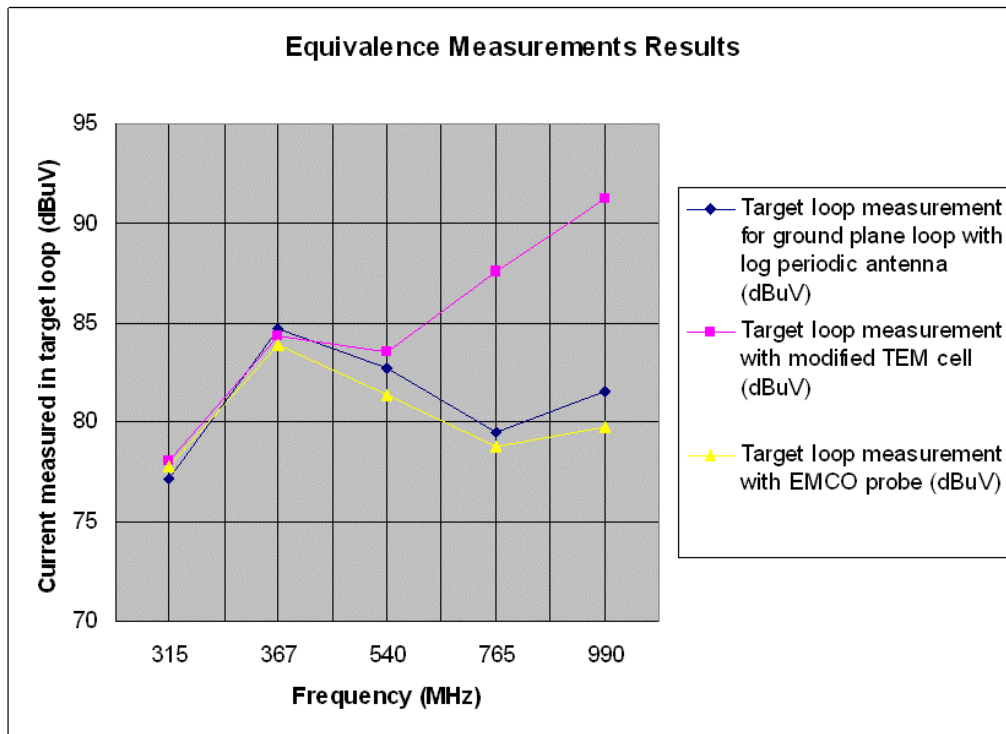


Figure 5-7: Graphic representation of the equivalence measurement results

6 Conclusions and Recommendations

Electromagnetic immunity tests form a critical part of the product development cycle. Linked to the stringent test requirements listed in applicable EMC test standards, e.g. IEC and Mil Standards are rigorous and expensive test methods. The fact that more than one iteration of EMC tests are often required prior to final EMC acceptance of the product imposes a heavy burden upon the total costs associated with overall product development. Therefore the need for less expensive, less time consuming, but still reasonably accurate pre-compliance EMC testing methods are sought. The focus of this thesis was therefore to investigate the equivalence between in-house and conventional EMI test techniques.

From the outset of the thesis the singular focus was to investigate the equivalence between in-house and conventional EMI test methods. From the equivalence discussion chapter it was evident that literature has been

produced addressing details on various techniques of performing EMI tests, for example E-field radiation and Bulk Current Injection (BCI).

To perform the BCI measurement it was decided to use the EMCO current probe. However, prior to performing the equivalence testing, the transfer impedance data of the EMCO probe was verified. A special CISPR 16 metal container was designed to perform the verification tests after problems were encountered with the initial test cabinet.

After the verification of the transfer impedance data, an in-house modified TEM cell was designed and constructed. The modified TEM cell design was based on a microstripline with an air dielectric substrate as opposed to the conventional Crawford cell. The reasons for following this route were:

1. Using the microstripline design provided some liberty in terms of the size of the test area within TEM cell.
2. The fact that the sentiment behind designing and constructing the modified Tem cell was to create a less expensive, easy to build, but yet effective in-house EMC measurement apparatus.

The modified TEM consists primarily of two areas, namely: the taper area and the uniform area. The purpose of the taper area is to ensure minimum loss of input signal prior to arrival at the uniform area. Various tapers exist, for example the Klopfenstein taper, Exponential taper, etc. However, for this investigation the exponential taper was chosen mainly due to its performance in the frequency band of interest ($BL \leq \pi$) compared to the other two options as per [6]. The main purpose of the uniform area is to provide a uniform E-field.

The process used in proving equivalence between the three test methods is summarised in Figure 5-1. Effectively it states that a two-fold process was followed, namely: 1. A process of calibrating both the TEM cell and EMCO probe in terms of the required levels of RF input power that will produce a current within the test loop equivalent to that produced by an E-field of 5V/m produced by the Log periodic antenna; 2. Once the calibration was done three measurements were performed and these were compared to each

other in an attempt to comment on the equivalence between the three methods. The test results revealed that both the TEM cell radiation method and the EMCO probe current injection method produce results that are equivalent within 0.9dB to that produced by the Log periodic antenna radiation method.

The final conclusion is that the research confirmed that in-house focused pre-compliance EMC test techniques can produce equivalent results to that of the more conventional techniques.

APPENDIX A

This appendix captures the Matlab code produced to plot the theoretical representation of the exponential taper's reflection coefficient.

```
% Theoretical Calculation and Plot of the S11 of an Exponential
taper
%Programmer: C.Nicholls

function [z]= test(f);      %Define a function with one input

w = 2.*pi.*f;
c = 3e8;
B=w./c;
Zl = 50;
Zo = 100;
L = 0.3;

S_11 = 0.5.* log(Zl/Zo).*((sin(B.*L))./(B.*L));

S_11=20*log10(abs(S_11));

plot(f/1e6,S_11,'b');grid;
xlabel('Frequency in MHz');
ylabel('Amplitude of S11 in dB')
title('Plot of S11 of Exponential taper')
```

APPENDIX B

This appendix captures the Matlab code produced to plot the theoretical versus measured representation of the exponential taper's reflection coefficient.

```
% M-file to Plot the theoretical and the measured S11 of the
constructed Exponential taper
%Programmer: C.Nicholls

function [z]= test(v1,f);

%Plot Theoretical S11
w = 2.*pi.*f;
c = 3e8;
B=w./c;
Zl = 50;
Zo = 100;
L = 0.3;

S_11 = 0.5.* log(Zl/Zo).*((sin(B.*L))./(B.*L));
S_11=20*log10(abs(S_11));
plot(f/1e6,S_11,'b');

hold on

%Plot measured S11
v1=20.*log10(abs(v1));
plot(f/1e6,v1,'r');grid;
axes(legend('Theoretical S11 of Tem Cell','Measured S11 of Tem
Cell'));
title('Plot of S11 of Exponential taper')
xlabel('Frequency in MHz');
ylabel('Amplitude of S11 in dB')

% hold off
```

APPENDIX C

This appendix captures the Matlab code produced to plot the uniformity measurements of the uniform area within the modified TEM cell.

```
% Code to calculate uniformity of a TEM cell using S21 measurements
% Programmer: C. Nicholls
```

```
function [z]=
test(v1,v2,v3,v4,v5,v6,v7,v8,v9,v10,v11,v12,v13,v14,v15,v16,v17,v18
,v19,v20,v21,v22,v23,v24,...

v25,v26,v27,v28,v29,v30,v31,v32,v33,v34,v35,v36,v37,v38,v39,v40,...
v41,v42,v43,v44,v45,v46,v47,v48,v49,...
v50,v51,v52,v53,v54,v55,v56,v57,v58,v59,...
v60,v61,v62,v63,v64,v65,v66,v67,v68,v69,...
v70,f);

format long e;
close all;
fs = 44100;
lengthof_S21 = 201;
j=1;

for i = 7:15:67

% Choosing the S21 MAGNITUDE measurement related to the chosen
frequency for FIRST round of measurements %
S21_Measurement1(1) = abs(v1(i));
S21_Measurement1(2) = abs(v2(i));
S21_Measurement1(3) = abs(v3(i));
S21_Measurement1(4) = abs(v4(i));
S21_Measurement1(5) = abs(v5(i));
S21_Measurement1(6) = abs(v6(i));
S21_Measurement1(7) = abs(v7(i));
S21_Measurement1(8) = abs(v8(i));
S21_Measurement1(9) = abs(v9(i));
S21_Measurement1(10) = abs(v10(i));
S21_Measurement1(11) = abs(v11(i));
S21_Measurement1(12) = abs(v12(i));
S21_Measurement1(13) = abs(v13(i));
S21_Measurement1(14) = abs(v14(i));
S21_Measurement1(15) = abs(v15(i));
S21_Measurement1(16) = abs(v16(i));
S21_Measurement1(17) = abs(v17(i));
S21_Measurement1(18) = abs(v18(i));
S21_Measurement1(19) = abs(v19(i));
S21_Measurement1(20) = abs(v20(i));
S21_Measurement1(21) = abs(v21(i));
S21_Measurement1(22) = abs(v22(i));
S21_Measurement1(23) = abs(v23(i));
S21_Measurement1(24) = abs(v24(i));
S21_Measurement1(25) = abs(v25(i));
S21_Measurement1(26) = abs(v26(i));
S21_Measurement1(27) = abs(v27(i));
S21_Measurement1(28) = abs(v28(i));
```

```

S21_Measurement1(29) = abs(v29(i));
S21_Measurement1(30) = abs(v30(i));
S21_Measurement1(31) = abs(v31(i));
S21_Measurement1(32) = abs(v32(i));
S21_Measurement1(33) = abs(v33(i));
S21_Measurement1(34) = abs(v34(i));
S21_Measurement1(35) = abs(v35(i));

% Choosing the S21 MAGNITUDE measurement related to the chosen
frequency for SECOND round of measurements %
S21_Measurement2(1) = abs(v36(i));
S21_Measurement2(2) = abs(v37(i));
S21_Measurement2(3) = abs(v38(i));
S21_Measurement2(4) = abs(v39(i));
S21_Measurement2(5) = abs(v40(i));
S21_Measurement2(6) = abs(v41(i));
S21_Measurement2(7) = abs(v42(i));
S21_Measurement2(8) = abs(v43(i));
S21_Measurement2(9) = abs(v44(i));
S21_Measurement2(10) = abs(v45(i));
S21_Measurement2(11) = abs(v46(i));
S21_Measurement2(12) = abs(v47(i));
S21_Measurement2(13) = abs(v48(i));
S21_Measurement2(14) = abs(v49(i));
S21_Measurement2(15) = abs(v50(i));
S21_Measurement2(16) = abs(v51(i));
S21_Measurement2(17) = abs(v52(i));
S21_Measurement2(18) = abs(v53(i));
S21_Measurement2(19) = abs(v54(i));
S21_Measurement2(20) = abs(v55(i));
S21_Measurement2(21) = abs(v56(i));
S21_Measurement2(22) = abs(v57(i));
S21_Measurement2(23) = abs(v58(i));
S21_Measurement2(24) = abs(v59(i));
S21_Measurement2(25) = abs(v60(i));
S21_Measurement2(26) = abs(v61(i));
S21_Measurement2(27) = abs(v62(i));
S21_Measurement2(28) = abs(v63(i));
S21_Measurement2(29) = abs(v64(i));
S21_Measurement2(30) = abs(v65(i));
S21_Measurement2(31) = abs(v66(i));
S21_Measurement2(32) = abs(v67(i));
S21_Measurement2(33) = abs(v68(i));
S21_Measurement2(34) = abs(v69(i));
S21_Measurement2(35) = abs(v70(i));

% Express S21_Measurement1&2 in db's %
S21_Measurement1=20*log10(S21_Measurement1);
S21_Measurement2=20*log10(S21_Measurement2);

% Calculating the maximum value of S21 measurements1&2 %
Normaliser1 = max(S21_Measurement1);
Normaliser2 = max(S21_Measurement2);

% Normalising measurements1 %
S21_Measurement1(1) = (S21_Measurement1(1)/Normaliser1);
S21_Measurement1(2) = (S21_Measurement1(2)/Normaliser1);
S21_Measurement1(3) = (S21_Measurement1(3)/Normaliser1);
S21_Measurement1(4) = (S21_Measurement1(4)/Normaliser1);
S21_Measurement1(5) = (S21_Measurement1(5)/Normaliser1);
S21_Measurement1(6) = (S21_Measurement1(6)/Normaliser1);
S21_Measurement1(7) = (S21_Measurement1(7)/Normaliser1);

```



```

S21_Measurement2(35) = (S21_Measurement2(35)/Normaliser2);

% Writing out the related frequency %
ftext = f(i)/1e6;
ftext = num2str(ftext);
ftext = ['frequency (MHz) =' ftext];

% Plotting figure %
figure (j)

% Create a vector consisting of the average of the two sets of
% measurements%

for n = 1:35
    S21_M=[S21_Measurement1(n) S21_Measurement2(n)];
    S21_Pos(n) = mean(S21_M);
end

% Create a 7x5 matrix corresponding to the physical measurement
performed %
m=1;

for l =1:5

    for k = 1:7

        S21_Matrix(k,l) = S21_Pos(m);
        m = m+1;
    end

end

% Plot the contour plot of the created 7x5 matrix %
surfc(S21_Matrix);
zlabel('S21 [dB]')
xlabel('Measurement points in direction A')

a=max(S21_Matrix);
b=max(a);

c=min(S21_Matrix);
d=min(c);

e=b-d;

max_diff = num2str(e);
max_diff = ['Maximum variation in amplitude [dB] =' max_diff];

k=max(a)+0.5;
l=max(a)+0.3;

text(1.5,1.5,k,ftext)
text(1.5,1.5,l,max_diff)

j=j+1;

end
j=1;

```

APPENDIX D

This appendix captures the Matlab code produced to plot the measured transfer impedance of the EMCO probe.

```
% M-file that converts the calculates and plot the measured
transfer impedance (Zt) of the EMCO probe
%Programmer: C.Nicholls

format long e;
close all;

% Load all S-Parameters in variable D
D = [v1];
a=1;
b=4;
%Extract individual S11-S22 from data

S=D(:, :);
S11=D(:, 1);
S21=D(:, 2);
S12=D(:, 3);
S22=D(:, 4);

%%Define numerators and denominators
den = (1-S11).*(1-S22)-S12.*S21;
num1=(1+S11).*(1-S22)+S12.*S21;
num2=2*S12;
num3=2*S21;
num4=(1-S11).*(1+S22)+S12.*S21;

%-----Determine Z-parameters-----
Z11=Z0*(num1./den);
Z21=Z0*(num2./den);
Z12=Z0*(num3./den);
Z22=Z0*(num4./den);

% % %-----Determine transfer impedance-----

Zt=Z21./(1+(Z22/50));

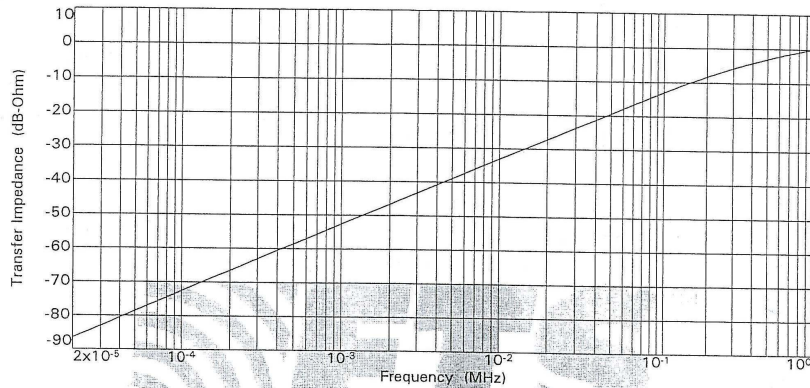
%Plot the Zt of the EMCO probe
figure(1);
loglog(f/1e6,abs(Zt),'m--')
grid;
title('Plot of Zt vs. Frequency');
xlabel('Frequency [MHz]');
ylabel('Zt [ohm]');
axes(legend('Zt of EMCO '));
```

APPENDIX E

The detail technical specifications of the EMCO current probe are captured in this appendix.



Transfer Impedance for Inductive Current Clamp
 Manufactured by EMCO
 Model Number: 94111-1L Serial Number: 50999



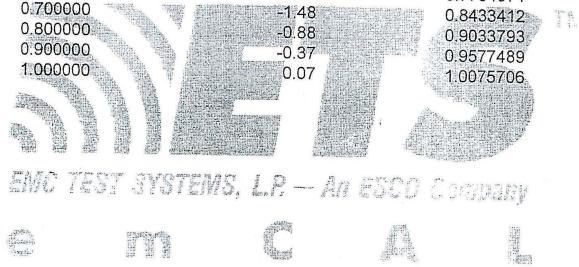
Frequency (MHz)	Transfer Impedance (dB Ohms)	Transfer Impedance (Ohms)
0.000020	-86.55	0.0000471
0.000050	-78.59	0.0001177
0.000100	-72.57	0.0002353
0.000500	-58.59	0.0011765
0.001000	-52.57	0.0023530
0.002000	-50.53	0.0029741
0.003000	-48.50	0.0037592
0.004000	-46.46	0.0047515
0.005000	-44.43	0.0060057
0.006000	-42.39	0.0075911
0.007000	-40.36	0.0095948
0.008000	-38.32	0.0121276
0.009000	-36.29	0.0153289
0.010000	-34.26	0.0193752
0.020000	-27.31	0.0430953
0.030000	-23.78	0.0647381
0.040000	-21.33	0.0858285
0.050000	-19.45	0.1065475

Transfer Impedance (dB Ohms) to be subtracted from receiver meter reading in dBV to convert to current dBA.
 Calibrated 14 Jun 00 (DD MMM YY).



Transfer Impedance for Inductive Current Clamp
Manufactured by EMCO
Model Number: 94111-1L Serial Number: 50999

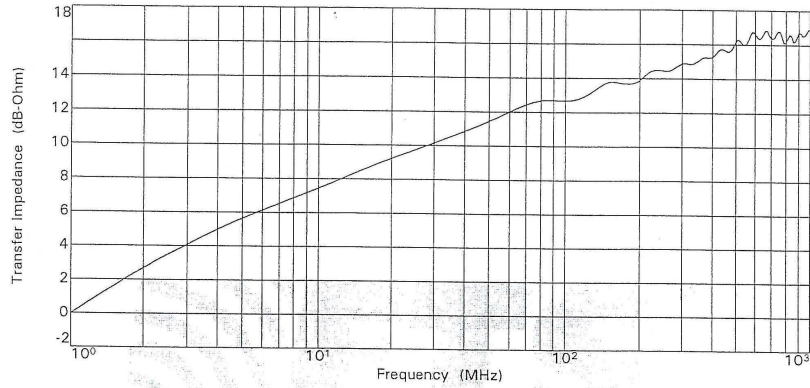
Frequency (MHz)	Transfer Impedance (dB Ohms)	Transfer Impedance (Ohms)
0.060000	-17.92	0.1270061
0.070000	-16.66	0.1469749
0.080000	-15.57	0.1665739
0.090000	-14.60	0.1861319
0.100000	-13.76	0.2050883
0.200000	-8.58	0.3725530
0.300000	-5.94	0.5047773
0.400000	-4.27	0.6114288
0.500000	-3.09	0.7002804
0.600000	-2.20	0.7764071
0.700000	-1.48	0.8433412
0.800000	-0.88	0.9033793
0.900000	-0.37	0.9577489
1.000000	0.07	1.0075706



Transfer Impedance (dB Ohms) to be subtracted from receiver meter reading in dBV to convert to current dBA.
 Calibrated 14 Jun 00 (DD MMM YY).



Transfer Impedance for Inductive Current Clamp
 Manufactured by EMCO
 Model Number: 94111-1L Serial Number: 50999



Frequency (MHz)	Transfer Impedance (dB Ohms)	Transfer Impedance (Ohms)
1.000000	-0.03	0.9964087
2.000000	2.68	1.3613117
3.000000	4.07	1.5985767
4.000000	4.98	1.7750313
5.000000	5.64	1.9134753
6.000000	6.13	2.0257402
7.000000	6.53	2.1198730
8.000000	6.86	2.2040155
9.000000	7.17	2.2818236
10.000000	7.44	2.3552307
20.000000	9.23	2.8924347
30.000000	10.15	3.2164458
40.000000	10.85	3.4867042
50.000000	11.45	3.7370590
60.000000	12.00	3.9790490
70.000000	12.42	4.1799193
80.000000	12.66	4.2940558
90.000000	12.69	4.3118313

Transfer Impedance (dB Ohms) to be subtracted from receiver meter reading in dBV to convert to current dBA.
 Calibrated 19 Jun 00 (DD MMM YY).



Transfer Impedance for Inductive Current Clamp
 Manufactured by EMCO
 Model Number: 94111-1L Serial Number: 50999

Frequency (MHz)	Transfer Impedance (dB Ohms)	Transfer Impedance (Ohms)
100.000000	12.67	4.3026890
110.000000	12.73	4.3294600
120.000000	12.93	4.4318331
130.000000	13.24	4.5931735
140.000000	13.57	4.7691951
150.000000	13.76	4.8754090
160.000000	13.77	4.8823842
170.000000	13.71	4.8476837
180.000000	13.68	4.8311196
190.000000	13.72	4.8529031
200.000000	13.89	4.9470493
225.000000	14.44	5.2710202
250.000000	14.45	5.2765945
275.000000	14.57	5.3527556
300.000000	14.87	5.5394991
325.000000	14.84	5.5214467
350.000000	15.05	5.6571716
375.000000	15.24	5.7833034
400.000000	15.28	5.8065877
425.000000	15.66	6.0651690
450.000000	15.67	6.0760971
475.000000	15.65	6.0626131
500.000000	16.18	6.4396038
525.000000	16.14	6.4110814
550.000000	16.04	6.3363266
575.000000	16.61	6.7706090
600.000000	16.63	6.7863770
625.000000	16.35	6.5663108
650.000000	16.64	6.7908633
675.000000	16.78	6.8992115
700.000000	16.41	6.6137633
725.000000	16.50	6.6820062
750.000000	16.78	6.9055752
775.000000	16.38	6.5880170
800.000000	16.15	6.4231503
825.000000	16.58	6.7451941

Transfer Impedance (dB Ohms) to be subtracted from receiver meter reading in dBV to convert to current dBA.
 Calibrated 19 Jun 00 (DD MMM YY).



Transfer Impedance for Inductive Current Clamp
Manufactured by EMCO
Model Number: 94111-1L Serial Number: 50999

Frequency (MHz)	Transfer Impedance (dB Ohms)	Transfer Impedance (Ohms)
850.000000	16.29	6.5275018
875.000000	16.31	6.5351606
900.000000	16.70	6.8403869
925.000000	16.60	6.7626953
950.000000	16.56	6.7309443
975.000000	16.82	6.9328819
1000.000000	16.91	7.0081836

Transfer Impedance (dB Ohms) to be subtracted from receiver meter reading in dBV to convert to current dBA.
Calibrated 19 Jun 00 (DD MMM YY).